CrossMark

ORIGINAL ARTICLE

Radiative effects of dust aerosol on West African climate using simulations from RegCM4

K. B. Raji[1] · K. O. Ogunjobi[2] · A. A. Akinsanola[2,3]

Abstract A regional climate model (RegCM4.4) has been used to investigate the dynamical effect of dust aerosol radiative forcing and its impact on West African climate. The simulations was performed with the non-dust aerosol version of the model (control) and a dust aerosol module for the year 2010. The spatial and temporal distribution of the aerosol optical depth (AOD) derived from the dust run was compared with observed aerosol data from Aerosol Robotic Network (AERONET) and other satellite products. The results from the simulations show that dust aerosol has a significant impact on West Africa Monsoon (WAM) system. The dust particles induced shortwave (SW) radiative forcing exerted a heating effect at the top of the atmosphere (TOA) over the study area during the DJF season and cooling in MAM. In contrast, the dust induced longwave (LW) radiative forcing exerted an atmospheric cooling during dry season of DJF. The LW radiative forcing at the TOA is maximum during JJA season with the core of 4.3 Wm^{-2} over the source region (Bodele). The highest degrees of correlation (r > 0.7) between modeled AOD and (AERONET, MODIS, OMI, and MISR) were observed over Cape Verde. Moderate (0.5 < r < 0.7) to poor correlations (r < 0.5) were also observed over Ilorin, Zinder, Dakar, Ouagadougou, Agoufou, and Banizoumbou. Further results over all the stations revealed that, RegCM4.4 underestimates AOD over Ilorin, Zinder, Cape Verde, Ouagadugou, Agoufou, and Banizoumbou when compared with AERONET and satellite observations except in Dakar where it overestimated AOD from MODIS. All the experiments exhibited a remarkable performance over Guinea and whole West Africa with low RMSE and high postive correlation.

Keywords Aerosol Optical Depth · West African Monsoon · Regional Climate Model · AERONET

Introduction

Dust aerosols have a critical effect on regional climate because of the large amount of dust particles emitted from arid and semiarid regions in the world (Huang et al. 2009; Shao et al. 2011; Tesfaye et al. 2013). Saharan desert, a region located north of West Africa, is the largest source region of dust in the world (Goudie and Middleton 2001). According to (Ozer 2001) an estimated 1600×10^6 tons of dust particles is lifted annually from the Sahara desert and transported westward by easterly winds. These aerosols are responsible for significant climate forcing through their direct effects on solar and thermal radiation and their indirect/semi indirect effects on cloud and precipitation processes (Shi et al. 2005; Huang et al. 2009). Furthermore, previous studies have shown that dust aerosol direct radiative effects have a significant impact on West African climate and are likely to play a role in modulating seasonal precipitation over the Sahel region. For instance, recent modeling studies suggest significant climatic effects of dust interacting with West African monsoon (WAM) dynamics from event to seasonal and climate scales (Miller et al. 2004; Konare et al. 2008; Perlwitz et al. 2010; Zhao et al.

✉ A. A. Akinsanola
  mictomi@yahoo.com; aakinsano2-c@my.cityu.edu.hk

[1] Department of Weather Forecast Services, Nigerian Meteorological Agency, Abuja, Nigeria

[2] Department of Meteorology and Climate Science, Federal University of Technology Akure, Akure, Nigeria

[3] School of Energy and Environment, City University of Hong Kong, Kowloon Tong, Hong Kong SAR

2011). Other analyses using satellite observations have similarly agree on the significant impact of dust on cloudiness and precipitation over Sahel (Klüser and Holzer-Popp 2010).

Recently, the rapid development of computational powers and numerical models have enabled the representations and simulations of atmospheric processes. The credibility and performance of these numerical models in the description of atmospheric processes can be evaluated based on the comparison between the simulations and observations. However, quantifying the large-scale atmospheric processes of dust particles as well as capturing the dust-climate interactions and feedbacks through field experiments or different observation techniques, is very challenging. In this regard, online coupled desert dust-climate models are a beneficial tool to simulate dust aerosol-radiation-climate interactions and feedbacks (Zhang 2010; Tummon 2011; Tesfaye et al. 2013). Global Circulation Models (GCMs) for instance, have been used to perform dust-climate simulations in order to examine the large-scale climatic variables which controls the dust load, long-range transportation and deposition (e.g., Yue 2009). The use of global scale desert dust-climate interactions and feedback mechanisms have also been reported in various studies (e.g., Mahowald et al. 2011; Rotstayn 2011; Gu et al. 2012; Sajani 2012). On the other hand, employing GCM, Woodward (2005) reported that in the future, due to the climate change induced desertification, the global burden as well as radiative influences of desert dust particles may considerably increase. The GCM dust-climate simulations generally provides vital informations on large-scale distribution and wide range of environmental roles of dust particles in the past, present and future. In global-scale models, because of their coarse grid resolution; there exists a large bias in simulated meteorological fields and surface variables (Croft et al. 2012). These biases may impose remarkable inaccuracies on computations of dust aerosol emission and atmospheric processes and consequently, in predicting the dust climatic effects (Darmenova and Sokolik 2007; Todd et al. 2008). In this respect, the desert dust module which is interactively coupled with high-resolution Regional Climate Model (RegCM) is a noteworthy tool to simulate a small-scale dust process, as well as its climatic effects with better accuracies (Gong et al. 2003; Wang 2004; Tummon et al. 2010; Konare et al. 2008; Solmon et al. 2008; Darmenova et al. 2009; Zhang et al. 2009; Giorgi et al. 2012).

Solmon et al. (2012) investigated the direct effect of dust aerosol on climate over West Africa using regional climate model (RegCM), with a specific focus on the Sahel region. They reported that the mean effect of dust over summer seasons was to reduce precipitation in majority of the Sahel region as a result of strong surface cooling and elevated diabatic warming inhibiting convection. However, on the very northern Sahel and in the vicinity of dust sources, a relative increase of precipitation was obtained as a result of enhanced diabatic warming in the lower atmosphere associated with high dust concentrations at low altitude. Zakey et al. (2006) implemented a dust module in a regional climate model (RegCM) to study the Saharan dust distribution and observed that the model reproduces the main spatial and temporal features of the dust distribution especially at seasonal timescale over the Saharan region. They concluded in there study that the coupled model is suitable for long-term simulation of dust effects on West African and European climate. In addition, Konare et al. (2008) used the same model (RegCM3) to simulate West African summer seasons and reported that; the radiative shortwave forcing of dust is to reduce the precipitation over the Sahel; strengthen the southern branch of the AEJ and weaken the Tropical Eastery Jet. Despite these wonderful studies, the distributions of dust aerosols and its impacts on climate are still not well understood. Therefore, this study assesses the potentials of Regional Climate Model (RegCM4.4) in quantifying the direct and indirect effects of dust aerosol radiative forcings on West African climate in the year 2010.

Design of the experiment

Study area

This study focuses on West Africa (0°–20°N) and (20°W–20°E) domain. The area where dust impact on climate and the various AERONET stations used for model validation are indicated (Fig. 1). The domain covers the major sources of dust aerosol in northern Africa, Guinea coast, and part of the Atlantic Ocean. The climate of the region is governed by the north–south movement of the Inter-tropical Discontinuity (ITD). The West Africa domain is divided into three climatic zones: Guinea coast (4°–8°N), Savannah (8°–11°N) and Sahel (11°–16°N) following the classifications defined in (Omotosho and Abiodun 2007; Abiodun et al. 2012; Akinsanola et al. 2015). Basically, the stations under study include: Ilorin-Nigeria (08°32′N, 04°34′E); Cape Verde-Tropical Atlantic Ocean (16°45′N, 22°57′W); Dakar-Senegal (14°42′N, 17°29′W); Banizoumbou-Niger (13°45′N, 02°39′E); Ouagadougou-Burkina Faso (12°22′N, 1°31′W); Agoufou-Mali (15°21′N, 1°29′W). The local climate of Ilorin, which is located at the northern boundary of the Guinea savannah region of Nigeria, is characterised by the north easterly wind known as harmattan which brings in air containing Saharan dust from the Chad basin. The climate is characterized by both wet and dry seasons. The mean monthly temperatures of Ilorin vary from 25–28.9 °C and total annual rainfall in the area is about 1200 mm. Dakar is located in a tropical region

Fig. 1 Study area used for dust simulations and AERONET observation sites at Banizoumbou (13°45′N, 02°39′E), Agoufou (15°21′N, 1°29′W), Ouagadougou (12°22′N, 1°31′W), and Ilorin (08°32′N, 04°34′E), Dakar (14°42′N, 17°29′W), and Cape Verde (16°N, 22°W)
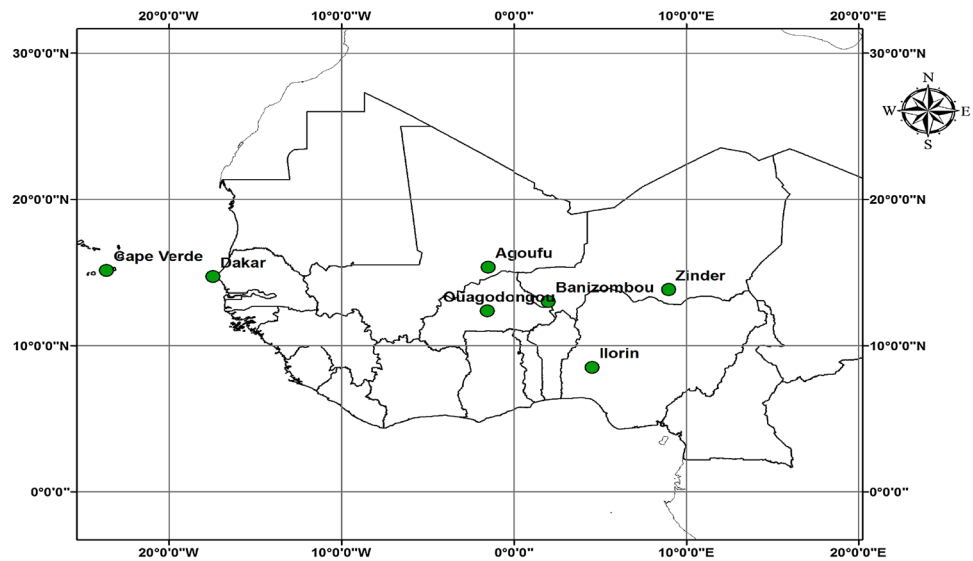
with well-defined dry and humid seasons resulting from the northeast winter winds and southwest summer winds. In Dakar, annual rainfall is about 600 mm between June and October, when maximum temperatures average 27 °C; December-February minimums are about 17 °C. Banizoumbou is located in the Sahel region, between the Sahara desert to the north and the Sudanian zone to the south. Banizoumbou is mainly influenced by sources located in Niger, south Algeria, Libya, and Chad with average annual rainfall of 450 mm. Over Cape Verde in the tropical Atlantic Ocean, the mean temperature range from 21 to 29 °C, and less than 250 mm annual rainfall. The local climate of Ougadougu is characterized by a mean temperature of 28 °C and annual rainfall of about 800 mm, while annual rainfall of 370 mm over Agoufu.

Observational data

AEROSOL ROBOTIC NETWORK (AERONET) surface observation network

AERONET is a ground-based remote sensing aerosol network established by NASA. In this study, aerosol optical depth (AOD) at 440 nm from seven sites over West Africa were used for comparison with model results. The sites are Banizoumbou (13°45′N, 02°39′E), Agoufou (15°21′N, 1°29′W) over Sudan region, Ouagadougou (12°22′N, 1°31′W) over Sahel region, and Ilorin (08°32′N, 04°34′E) over the southern biomass burning region, Dakar (14°42′N, 17°29′W) at the coast, and Cape Verde (160°N, 220°W) on a near-coast island. All of the retrievals of AOD are quality level 2, and the uncertainty of AOD measurements is about

±0.01 (Holben et al. 2001). Detail description of instruments used can be found in Holben et al. (1998).

Moderate Resolution Imaging Spectroradiometer (MODIS)

The Moderate Resolution Imaging Spectroradiometer (MODIS) instruments on board the NASA Terra and Aqua platforms are uniquely designed with wide spectral range, high spatial resolution, and near daily global coverage to observe and monitor the Earth changes including tropospheric aerosols (Kaufman et al. 1997). The MODIS instruments provide observations at moderate spatial resolutions (1–250 km) and temporal resolutions (1–2 days), over different portions of the electromagnetic spectrum. Therefore, in this study, the retrieved "deep blue" AOD at 440 nm from MODIS-Terra level 2 is used for monthly mean AOD validation over all the stations under study.

Multi-angle Imaging Spectroradiometer (MISR)

The MISR has a temporal resolution of 16 days and nominal spatial resolutions of 250, 275 m, and 1 km, but radiances at 1.1 km resolution are processed to yield the standard Level-2 MISR aerosol product at a 17.6 km×17.6 km pixel size. The MISR-AOD retrievals (level-3 data) have a higher grid resolution (0.5°×0.5°) in comparison to the Moderate Resolution Imaging Spectroradiometer (MODIS) of Level-3 which has the resolution of 1°×1°. In this study, Terra MISR monthly-averaged datasets at (0.5°×0.5°) spatial resolution are utilized to evaluate the simulated results over the whole domain of interest.

Ozone monitoring instrument (OMI)

The OMI has a nadir-viewing imaging spectrometer that measures the top of the atmosphere (TOA) upwelling radiances in the ultraviolet and visible regions of the solar spectrum (270–500 nm). The OMI was originally designed to retrieve data on trace gasses such as O_3, NO_2, SO_2, etc., but it also provides valuable information on atmospheric aerosols. It has a wavelength range around 400 nm that can be used to detect elevated layers of absorbing aerosols such as those resulting from biomass burning and desert dust plumes.

Tropical rainfall measuring mission (TRMM)

This earth observation satellite measure rainfall and latent heat of condensation exchange over the tropical and subtropical regions. The precipitation data used in this study are on a daily temporal resolution and a $0.25° \times 0.25°$ spatial resolution extending from 0°S to 20°N latitude (Huffman et al. 2001 and 2007). The positive biases in TRMM 3B-42 over Africa tropical forest occur mainly during the dry season (Adeyewa and Nakamura 2003).

ERA-INTERIM reanalysis data

These data are global reanalysis dataset produce by European Centre for Medium-Range Weather Forecasts (ECMWF) covering the period from 1989 to present. Data are gridded and available at various spatial resolutions and 37 vertical pressure levels. The reanalyses datasets used in this study were daily mean, gridded at $0.5° \times 0.5°$ in space and spanned across the West Africa domain.

Model description

This study employs the regional climate model version 4.4 (RegCM4.4) developed at the International Center for Theoretical Physics (ICTP) due to its wide applications in regional climate and environmental change studies (Giorgi et al. 2012). Keeping the same basic model dynamics as in RegCM3, RegCM4 is a hydrostatic, compressible, sigma-p vertical coordinate model run on an Arakawa B-grid, in which the wind and thermo dynamical variables are horizontally staggered. The dust scheme of RegCM4 represents the dry dust particle size distribution through size bin approach. The whole-size spectrum of dust particles covers a diameter range of 0.01–20.0 m,

divided into four size-bins, namely, the fine (0.01–1.0 m), accumulation (1.0–2.5 m), coarse (2.5–5.0 m), and giant (5.0–20.0 m) particle size modes (Zakey et al. 2006). Using prognostic dust bin concentrations, long-wave refractive indices, and absorption cross sections, the dust particles long-wave emissivity/absorptivity influences are implemented based on Solmon et al. (2008). Accordingly, the model computes the shortwave radiative influences of all the above aerosol types using these optical properties, along with the long-wave effects of dust particles (Giorgi et al. 2012). More information on different aspects of RegCM4-aerosol model is described in Giorgi et al. (2012).

Dust experimental design

The initial and boundary conditions were considered from ECMWF, Era-Interim reanalysis data. The lateral boundary conditions are updated every 6 h. Grell scheme closure is used in the simulation to describe moist convection. The topographic and vegetation datasets (GTOPO30) and default land use types were from the Global Land Cover Characterization (GLCC) respectively. The model horizontal resolution is 50 km. The domain center is (10.0°N, 2.0°E) with 120 grid cells in the W–E direction and 80 in the N–S direction. The model domain covers West Africa (20°W–20°E, 0°–25°N), and the simulation was performed from Jan 1, 2009, to Dec 31, 2010; the first year (2009) was considered as spin up. It is worthy to note that the choice of the year 2010 is because of the occurrence and persistent of high dust loading over the West African region.

The first experiment was carried out (label: control) without allowing the natural and anthropogenic dust aerosol to interact with the meteorological field (No dust). In the second experiment (label: I- direct1), the interaction is allowed through the perturbation of the radiation field by dust aerosol, so the response of the atmospheric thermodynamic field to the direct aerosol radiative forcing can be examined i.e. dust without radiation feedbacks. Lastly, the third experiment (label: I- direct2) was carried out considering dust aerosols with radiation feedbacks.

The observational datasets described above were used in this study for comparison and validation of simulated results. This enables a comprehensive analyses of the spatiotemporal distribution of dust AOD, seasonal and inter-annual variations of AOD, and as well as the radiative effect of aerosols on the climate of West Africa. The model validation and intercomparison with the ground and satellite-based observations were carried out using

required statistical analysis such as the Pearson's correlation coefficient. Standard deviation, root mean square error, mean bias error, and coefficient of efficiency. The backward trajectories traced by the NOAA Hybrid Single Particle Lagrangian Integrated Trajectory (HYSPLIT)

model of days with maximum dust load based on AERONET daily observations were plotted with endpoints in Dakar, Cape Verde, and Banizoumbou, and time step was 6 h for 108 h (5 days).
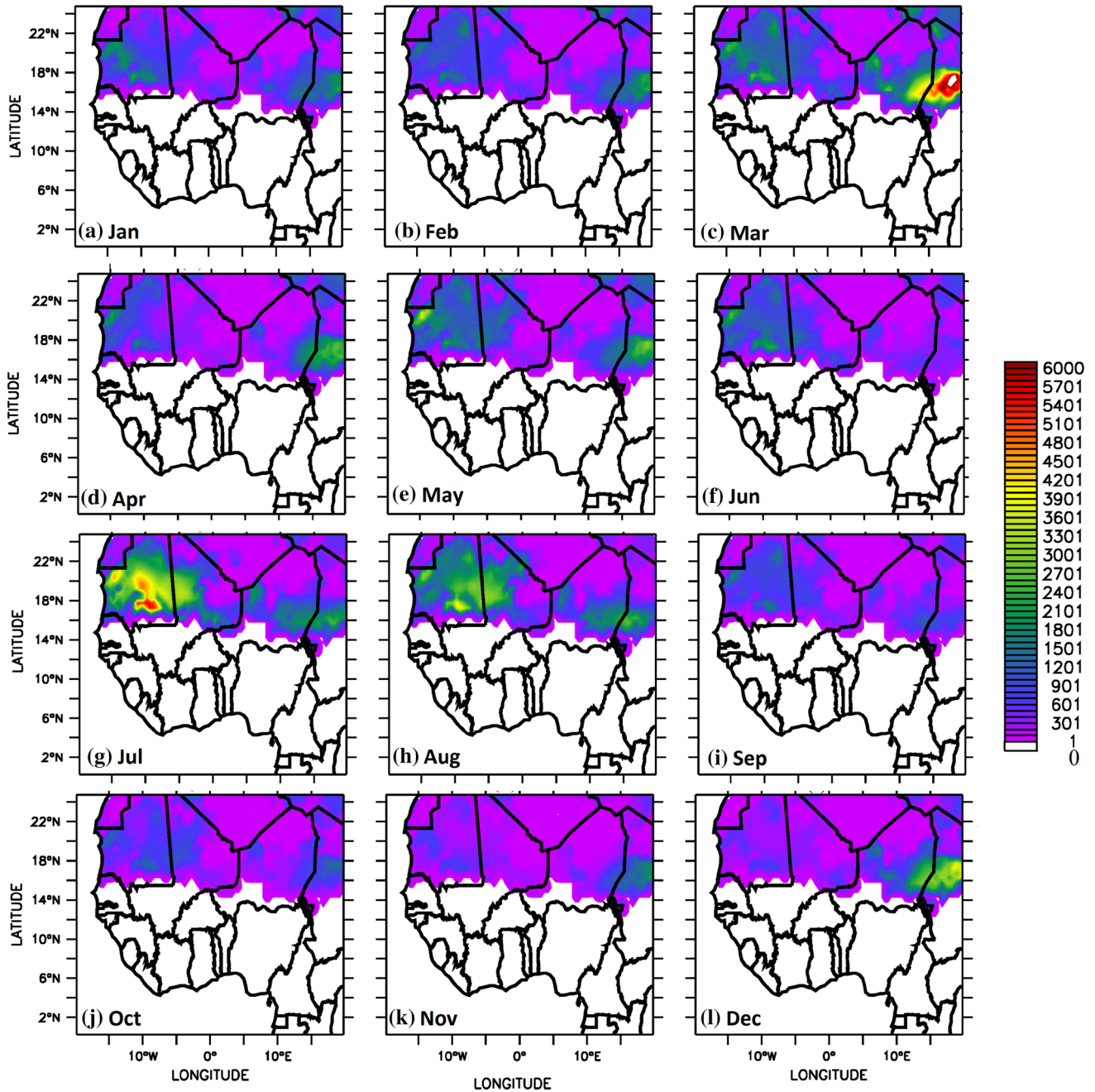

Fig. 2 Dust monthly mean emission (µg/kg) showing dust sources and their seasonal activities for 2010

Results and discussion

Dust emission, distribution, deposition, transport and trajectories

The distribution of dust concentration over the study area as shown in Fig. 2 revealed the different dust sources based on the concentration. RegCM4 captured few different sources with high dust concentration and emissions such as Bodele depression and some isolated sources in West Africa (Prospero 2002; Ginoux et al. 2012). The seasonal scale of dust concentration showed that the Bodele source which extended from Niger to Chad is predominant only between March and December with the maximum activity in March (Fig. 2). This source activity reported by RegCM4 is consistent with the maximum activity length from January to March reported by Washington and Todd (2005). The isolated sources, located over Mauritania and Mali regions of West Africa, as observed by RegCM4 were active between July and August with the maximum activity in July.

The spatial distribution of seasonal mean dry deposition fluxes of mineral dust for 2010 across the study region is shown in Fig. 3. During the dry season between November and March, it was observed that dust deposition source like Bodele depression extends to other areas like Niger and Chad in the Sahara region of West Africa. However, during the monsoon period between June and September, dry dust deposition was more defined and covers a larger area of the region. There was a shift in the position of maximum dry deposition to Mauritania and Mali during June–July–August (Chiapello et al. 1995). In RegCM4, no dry deposition was found in the Gulf of Guinea even though four types of dust particles size were considered in the experiment configuration of this study. The wet deposition processes over West Africa were also parameterized in RegCM4 as shown in Fig. 4. The seasonal pattern of the dust wet deposition was analyzed for this region. Results showed that dust wet deposition pattern varies with season, highest deposition during the wet season and its driven by the ITD dynamics. It was observed that no wet deposition fluxes occur over the whole region during the dry months (DJF). However, in the months of March-April-May, there was an increasing wet deposition flux over Guinean coast as a result of increasing rainfall in the coastal
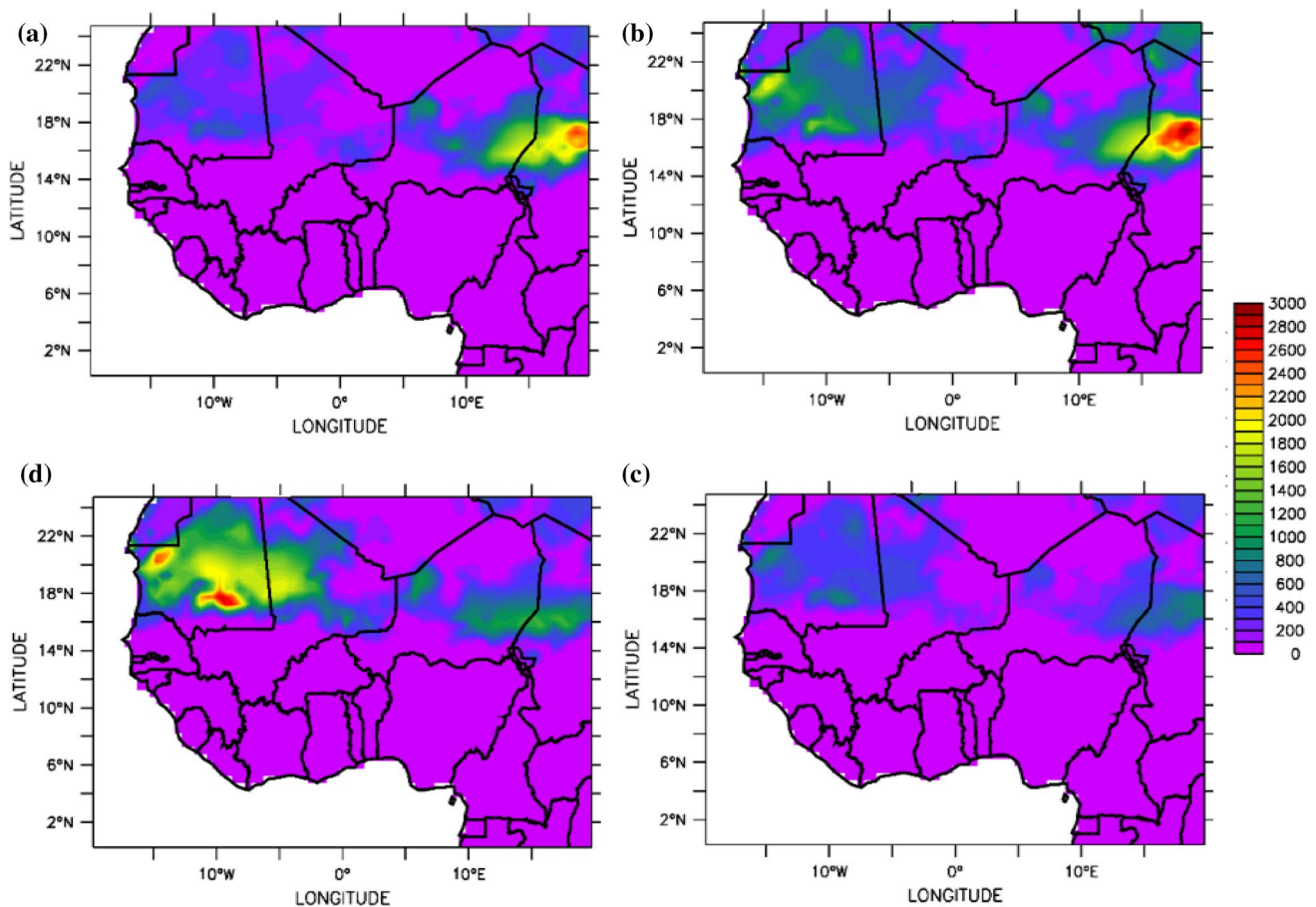

Fig. 3 Seasonal distribution of dry deposition flux (mg/m^{2}day) for **a** DJF **b** MAM **c** JJA **d** SON for 2010
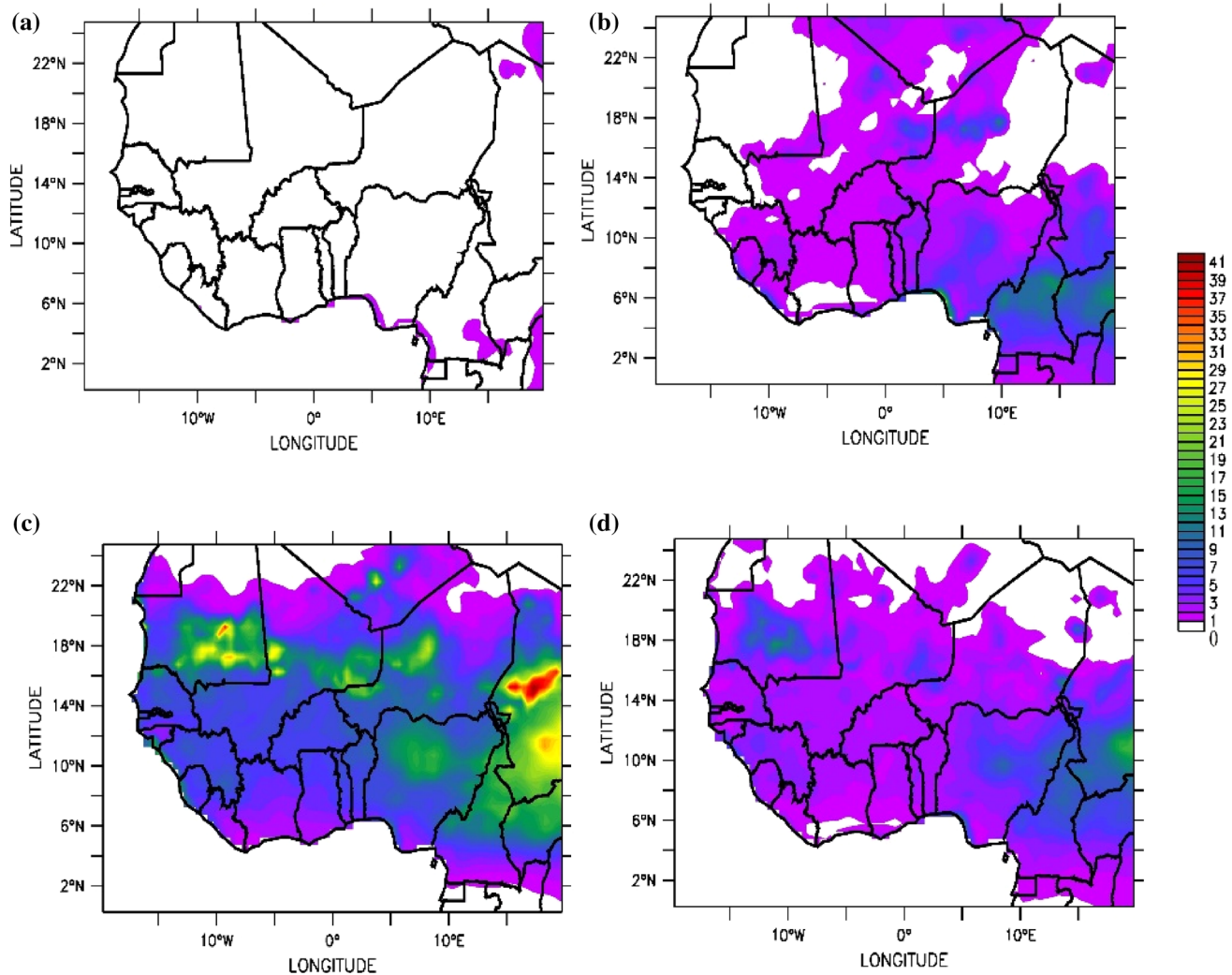
Fig. 4 Seasonal distribution of wet deposition flux (mg/m²day) for **a** DJF **b** MAM **c** JJA **d** SON for 2010
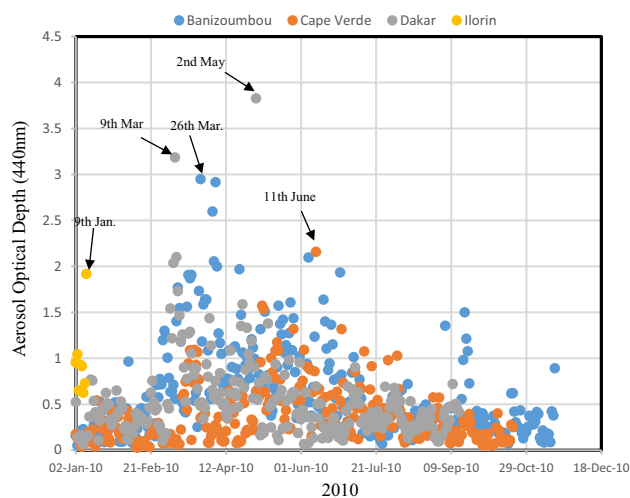

Fig. 5 Daily averages of AERONET Aerosol Optical Depth ($\lambda = 440$ nm) observations from January–December, 2010

regions. Maximum depositions of dust over West Africa were predominant in JJA. Measurements of dust deposition have been conducted with traps over land and Ocean but are generally few and incomplete, particularly for dry deposition. For example, McTainsh et al. (1999) measured deposition rates of about 200 g/m²year (~547 mg/m²day) in Niger which is found to be lower than that simulated by RegCM4. Figure 5 shows the daily averages of AOD at wavelength of 440 nm from January to December, 2010 over some selected AERONET stations in West Africa. It was observed that there were large variations in the distribution of aerosol particles in these areas. Over Banizoumbou, the maximum AOD was observed on 26th March and 5th April, Cape Verde showed the maximum AOD in 11th June while, that over Dakar was observed on the 9th March and 2nd May. These dates observed as the maximum AOD over the selected stations formed the basis by which the
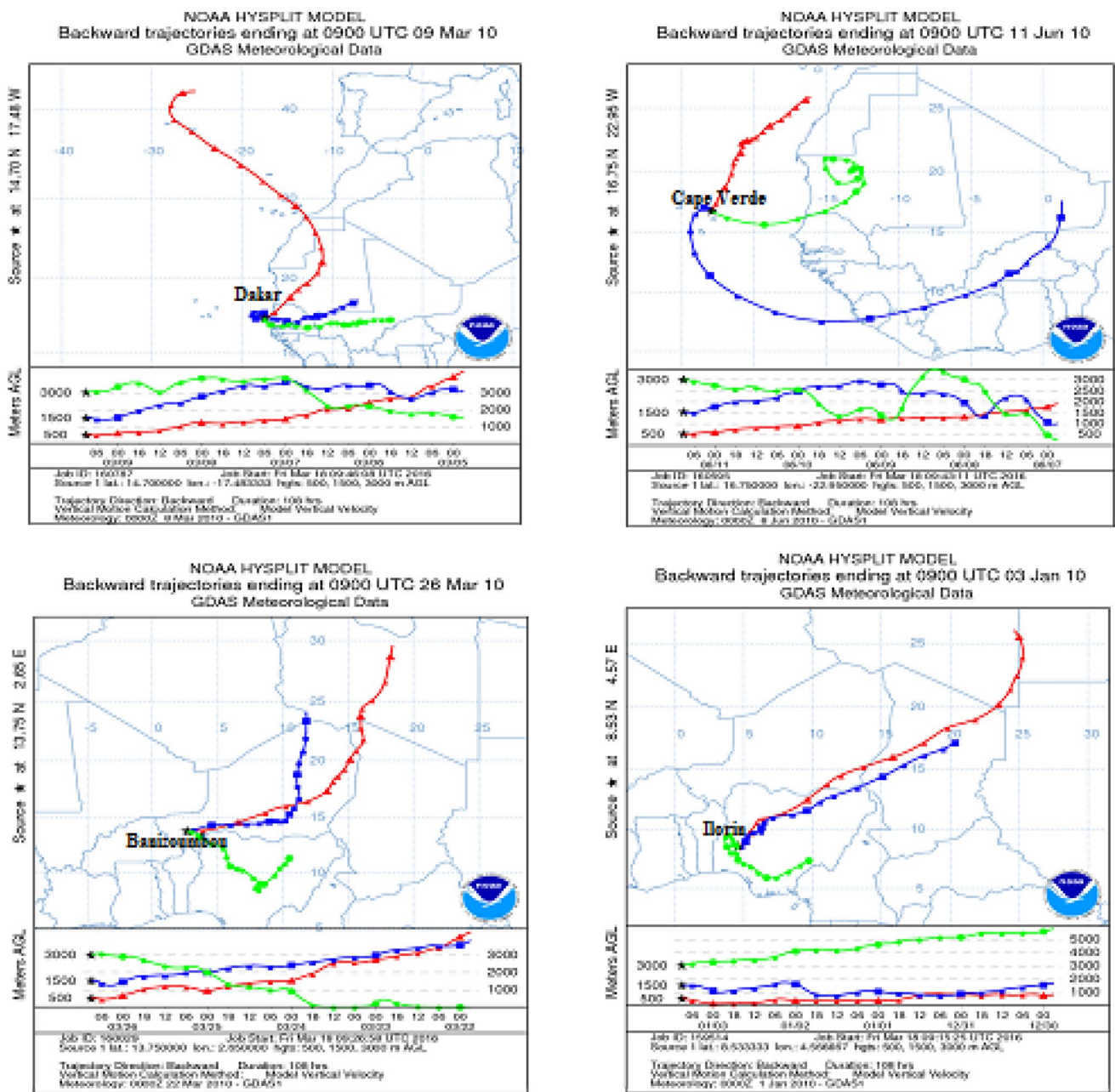
Fig. 6 5-day backward trajectories traced by the NOAA Hybrid Single Particle Lagrangian Integrated Trajectory (HYSPLIT) model over Dakar, Cape Verde, Banizoumbou, and Ilorin

back trajectories by HYSPLIT model were plotted in order to trace the origins of the aerosol loads.

The backward trajectories traced by the NOAA Hybrid Single Particle Lagrangian Integrated Trajectory (HYSPLIT) model with endpoints in Dakar, Cape Verde, and Banizoumbou and Ilorin for 09:00 UTC are shown in Fig. (6). The trajectories of days with maximum aerosols concentration (Fig. 5) based on AERONET AOD daily observations were plotted for each station, and time step

was 6 for 108 h (5 days). At the bottom of each map, back trajectories are represented for the following atmospheric heights: 500 m (red), 1500 m (blue) and 3000 m (green). These curves represent the height of the air mass during particle transport. Trajectories corresponding to other dates with rich dust aerosols were found to be similar. The trajectories show that the air masses reaching Dakar and Cape Verde from the lowest level at 500 m up to 2000 m originated from the Senegal, Mauritania, and Mali areas. The

high altitude (from 3000 m and beyond) long-range aerosol particles ending at these stations originated from the Mediterranean Sea. The air masses carrying atmospheric aerosols reaching the coastal and Island stations are generally from the maritime environment and other contributions from the continental sources like burning of biomass and fossils, and dust particles from the Sahara deserts which has also been reported by Prospero (2002) and Ogunjobi and Kim (2008).

The trajectories arriving Banizoumbou and Ilorin from the surface at 500 m to about 2000 m originated mainly from the Sahara desert of Northern Africa which has been identified as the major source area of dust loads (Prospero 2002). At higher altitude from 3000 m and beyond, the air masses reaching these areas which are majorly

characterized by heavy biomass burning originated from the continental sources of the Savannah region.

The seasonal mean spatial distributions of dust aerosol Short-Wave Surface Radiative Forcing (SWSRF) are shown in Fig. 7. The simulation results show that the dust aerosol SWSRF varied during the entire year over West Africa. It was observed that dust- induced radiative forcing is negative at the surface with minimum values ≥40 W/m^2 over the source region during the summer monsoon season. Moreover, the seasonal mean spatial distributions of dust aerosol Long-Wave Surface Radiative Forcing (LWSRF) is shown in Fig. 8. The dust aerosols interactions with LW radiation (especially aerosols with large sizes) as well as their emission of thermal radiation jointly induce an enhancement in the net surface LW radiative flux at the surface which is
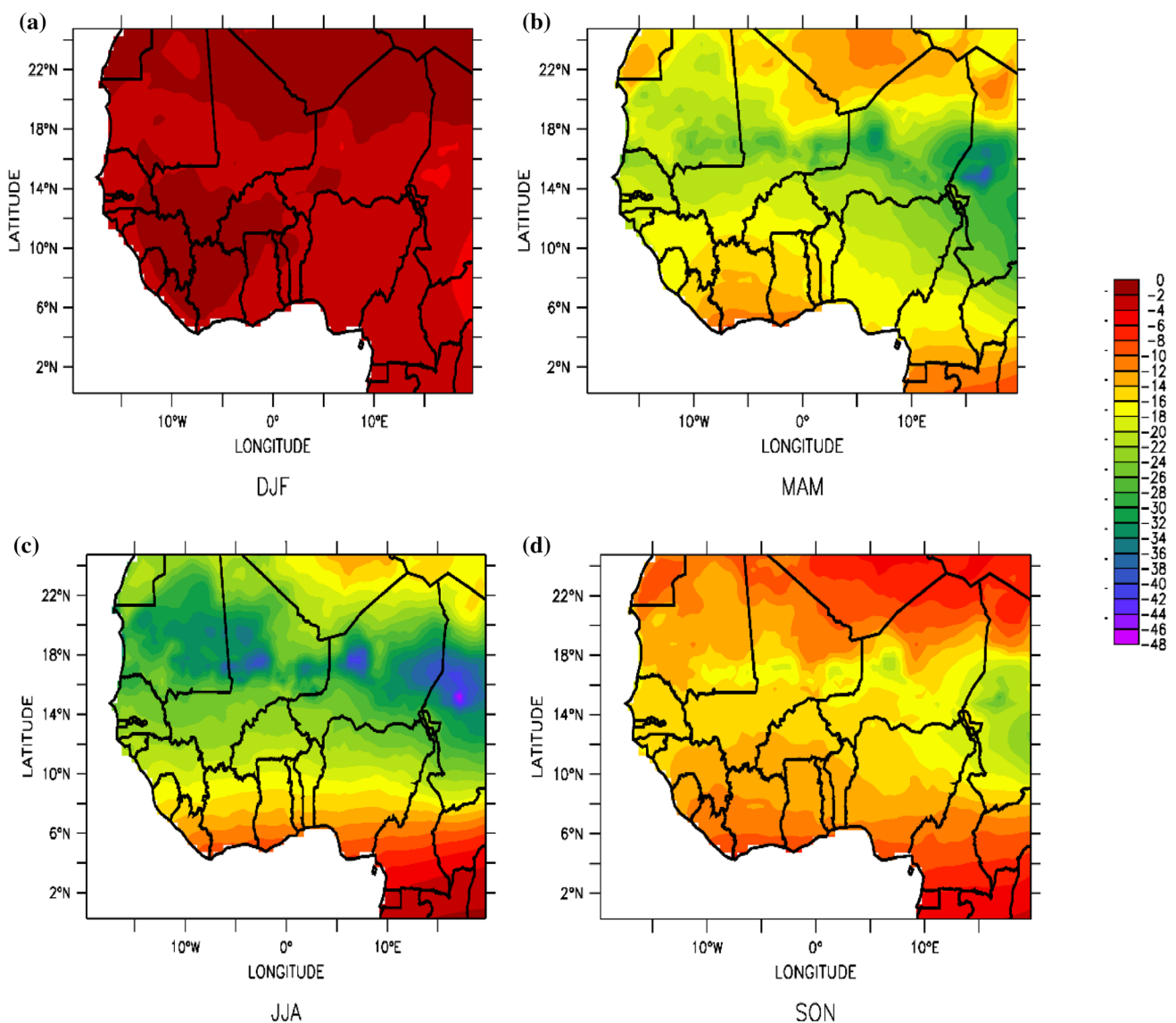

Fig. 7 Dust induced Shortwave Surface Radiative Forcing (W/m^2) at the top surface for **a** DJF **b** MAM **c** JJA **d** SON for 2010
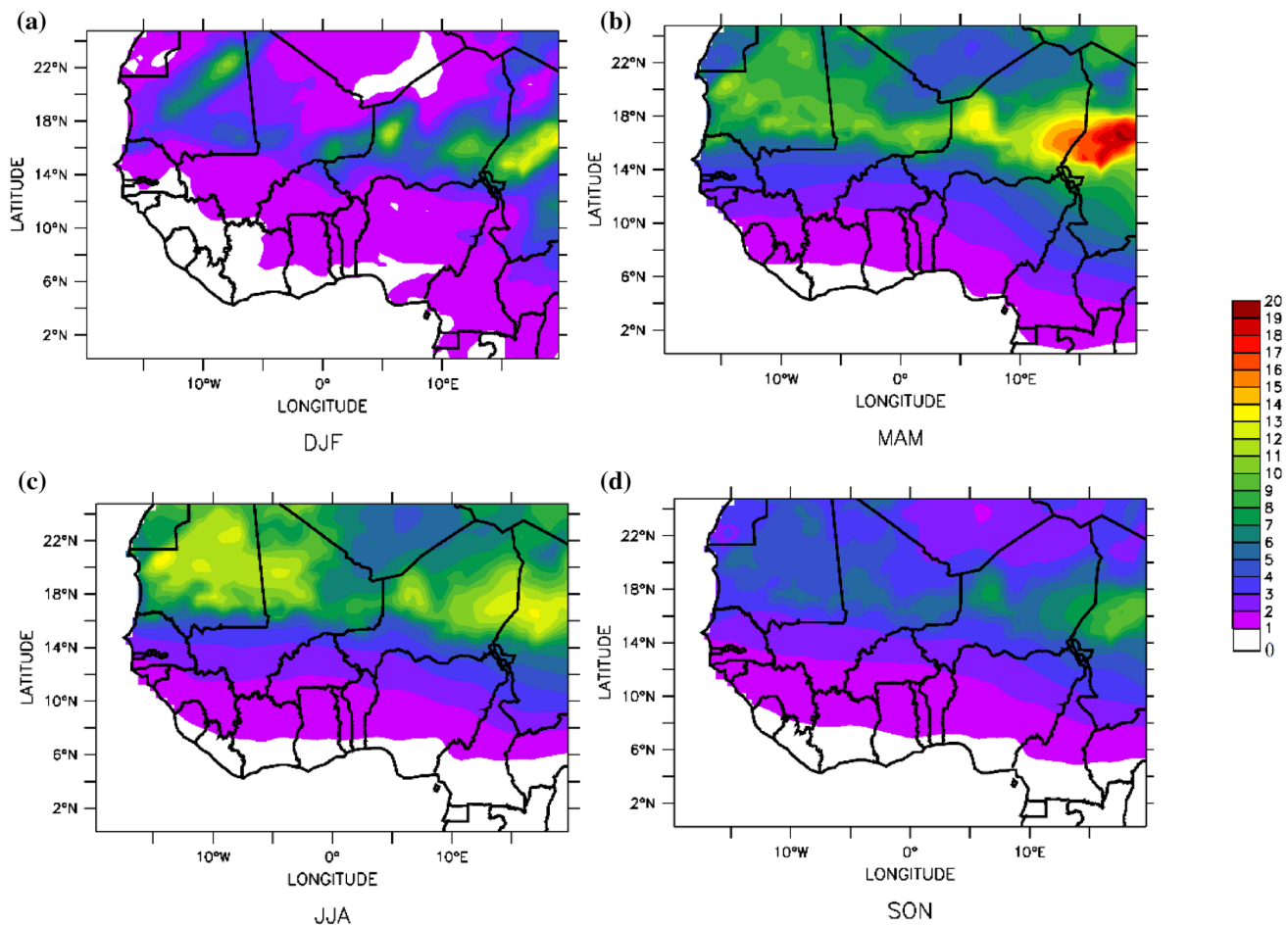
Fig. 8 Dust induced Longwave Surface Radiative Forcing (W/m²) at the top surface for **a** DJF **b** MAM **c** JJA **d** SON for 2010

observed to be opposite to SWSRF. It was found that the LWSRF was positive throughout the year which indicates the warming effect of dust over West Africa. Maximum LWSRF coincides with the transition period between the dry and wet season with values reaching 20 W/m² over the source region during MAM. Furthermore, the Net Surface Radiative Forcing (NSRF) (i.e. difference between SWSRF and LWSRF) exhibits similar spatial and seasonal pattern with observations of SWSRF but a considerable rise with minimum value reaching -36W/m² over the source region during JJA (Fig. 9). The negative values of SWSRF and NSRF indicate that dust exerts essentially a cooling effect independently of the season with the maximum during JJA over West Africa. The seasonal radiative forcing obtained for both SWSRF and NSRF during JJA are in agreement with Solmon et al. (2008, 2012), Malavelle et al. (2011) Konare et al. (2008).

The seasonal mean spatial distributions of dust induced Shortwave and Longwave radiative forcing at the top of the atmosphere are presented in Figs. 10 and 11

respectively. The dust -induced SW top of the atmosphere radiative forcing showed both warming and cooling effect during the year. Significantly, the dust induced radiative forcing at the TOA decreased to negative values towards south of 15°N in MAM, JJA, and SON. This is due to the changes in surface albedo, from the desert in the North to the Sudanian savannas in the South and reduction in dust loading quantity. The SW radiative forcing at the TOA is minimum during JJA over land (-9 to -15 Wm^{-2}), with maximum values (varying between 1 and 9 Wm^{-2} during MAM as shown in Fig. 10. The induced SW radiative forcing at the TOA gives a heating effect in the study area during DJF. In contrast, the LW radiative effects exhibit atmospheric radiative cooling. The spatial-seasonal distribution of LW radiative forcing decreased from zero to negative -0.8 Wm^{-2} at the TOA during DJF as shown in Fig. 11. However, the LW radiative forcing at the TOA is maximum during JJA with the maximum value of 4.3 Wm^{-2} over the source region. The simulation further shows that the magnitude of SW radiative forcing at the
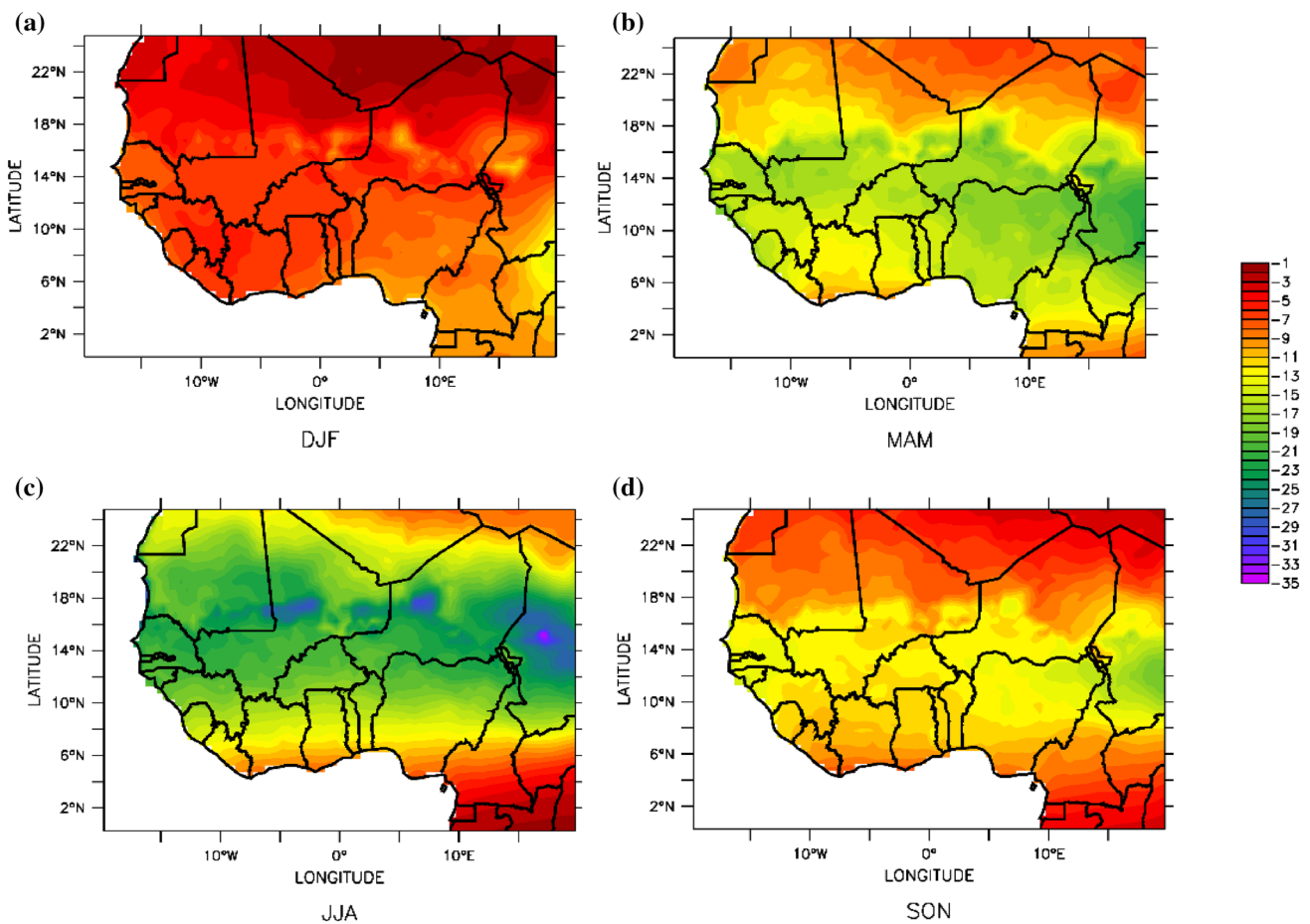
Fig. 9 Dust induced Net Surface Radiative Forcing (W/m^2) at the top surface for **a** DJF **b** MAM **c** JJA **d** SON for 2010

TOA is ~1 to 2 times higher, for warming and ~10 times higher for cooling, than that of the LW radiative forcing values (Tesfaye et al. 2015). Figure (12) further shows the dust induced net radiative forcing at the Top of the Atmosphere (TOA). It was observed that the Net radiative forcing at the TOA due to dust presence are generally negative over vegetated areas and positive over the desert regions of West Africa. The positive value of Net radiative forcing over the desert might be due to the high albedo values of desert and dust SW absorption. The change of sign of dust net radiative forcing along 16°N is due to a sharp decrease in surface albedo between the Sahara desert in the north and the Sudanian savannah in the south. It may also be attributed to the decrease of dust loading away from the source regions. These findings suggest that dust direct radiative effect at the TOA is essentially cooling especially over vegetation areas, and warming effect over desert regions which is in agreement with previous research of Solmon et al. (2008, 2012).

RegCM4 simulated West Africa Monsoon (WAM) features

The spatial distribution the December-January-February (DJF) pattern of rainfall is shown in Fig. 13(a–d). The rainfall distribution was observed only south of 10°N in this period, with the peak of rainfall (between 9 mm and 10 mm) along the Guinea coast (12°E–12°W). Similar distribution was observed in the summer monsoon months of June–September, but a wider coverage of maximum rainfall majorly along the Guinea coast was observed (Fig. 14). The core of the maximum rainfall was observed over Fouta Djallon and Cameroun Mountain. The modeled rainfall maximums were consistent with the TRMM observation in all the periods, although RegCM4 exhibited noticeable bias especially over the western parts of the study area.

In addition, the rainfall distribution exhibits a meridional gradient, with rainfall decreasing in amount from the southern part of West Africa to northern parts (Sahel) in
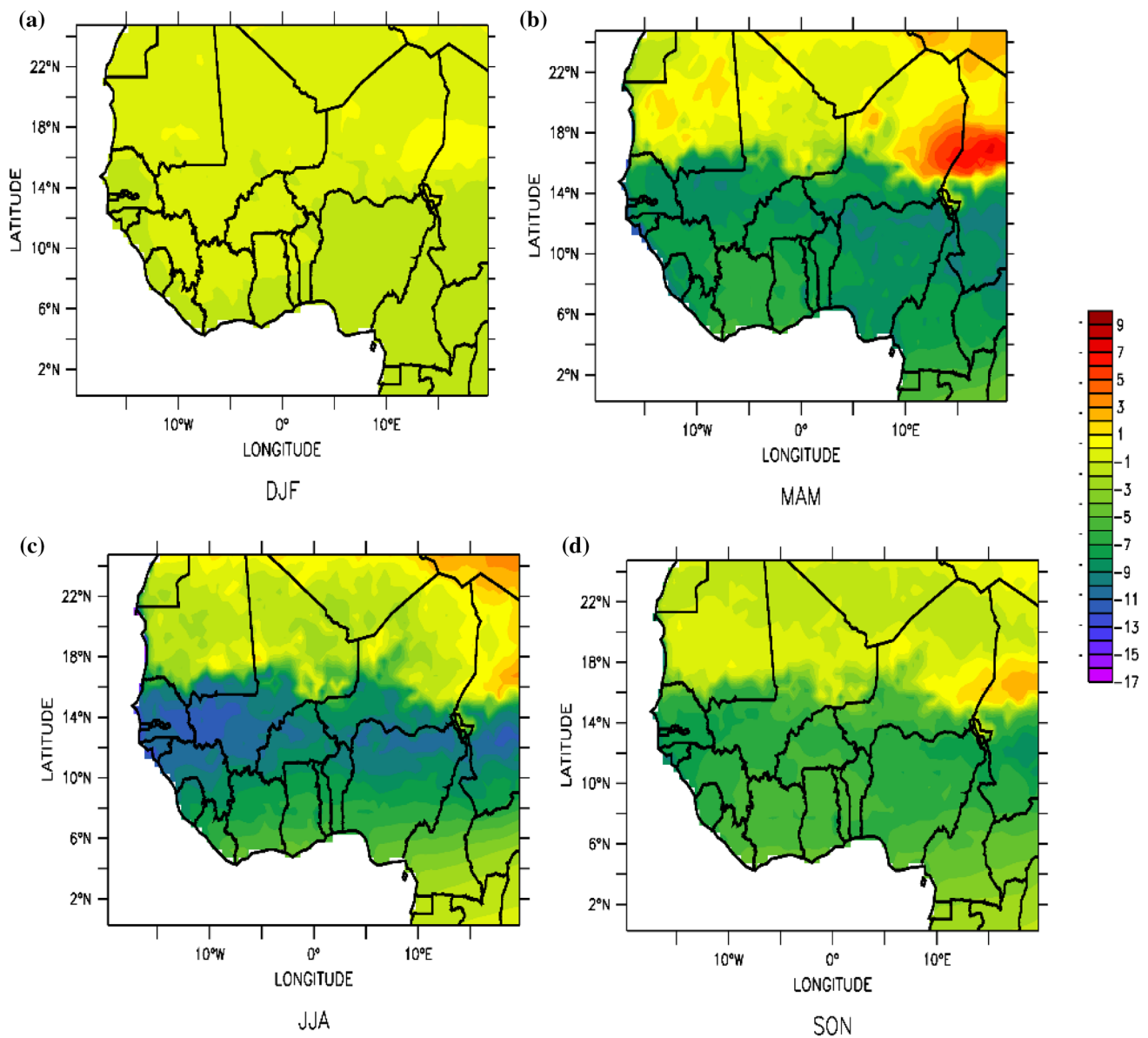
Fig. 10 Dust induced Shortwave Radiative Forcing (W/m2) at the TOA for **a** DJF **b** MAM **c** JJA **d** SON for 2010

association with the latitudinal migration of the ITD. Generally, the dust aerosol induced RegCM4 run tends to overestimate orography associated rainfall along the Guinea highlands and Jos plateau.

Figure 15 shows the Taylor diagram of simulated 2010 rainfall correlation coefficient, root mean square deviation and standard deviation calculated with regards to TRMM observations. Statistics are calculated over the Guinea, Savannah and Sahel, and represent simulations performed in the different experiments, including dust (DUST-RAD), (DUST + RAD) or not (−CTRL). It was observed that, the simulated results of all the experiments were consistent with the TRMM observations with the correlation

coefficient >0.95 in all stations (15a–c). Furthermore, over the Guinea, the dust aerosol induced run rainfall slightly deviated away with the standard deviation higher than the observed data. However, RegCM4 experiments showed good performance over Guinea with low RMSE (Fig. 15a). A significant difference between RegCM4 control output and TRMM was found over Savannah zone with the highest standard deviation than other experiments (Fig. 15b). Figure 15b also showed a low performance of RegCM4 due to high RMSE especially in the control case when compared with the observed over the Savannah zone. In the case of Sahel (Fig. 15c), a large difference was found between TRMM and RegCM4 dust with radiative
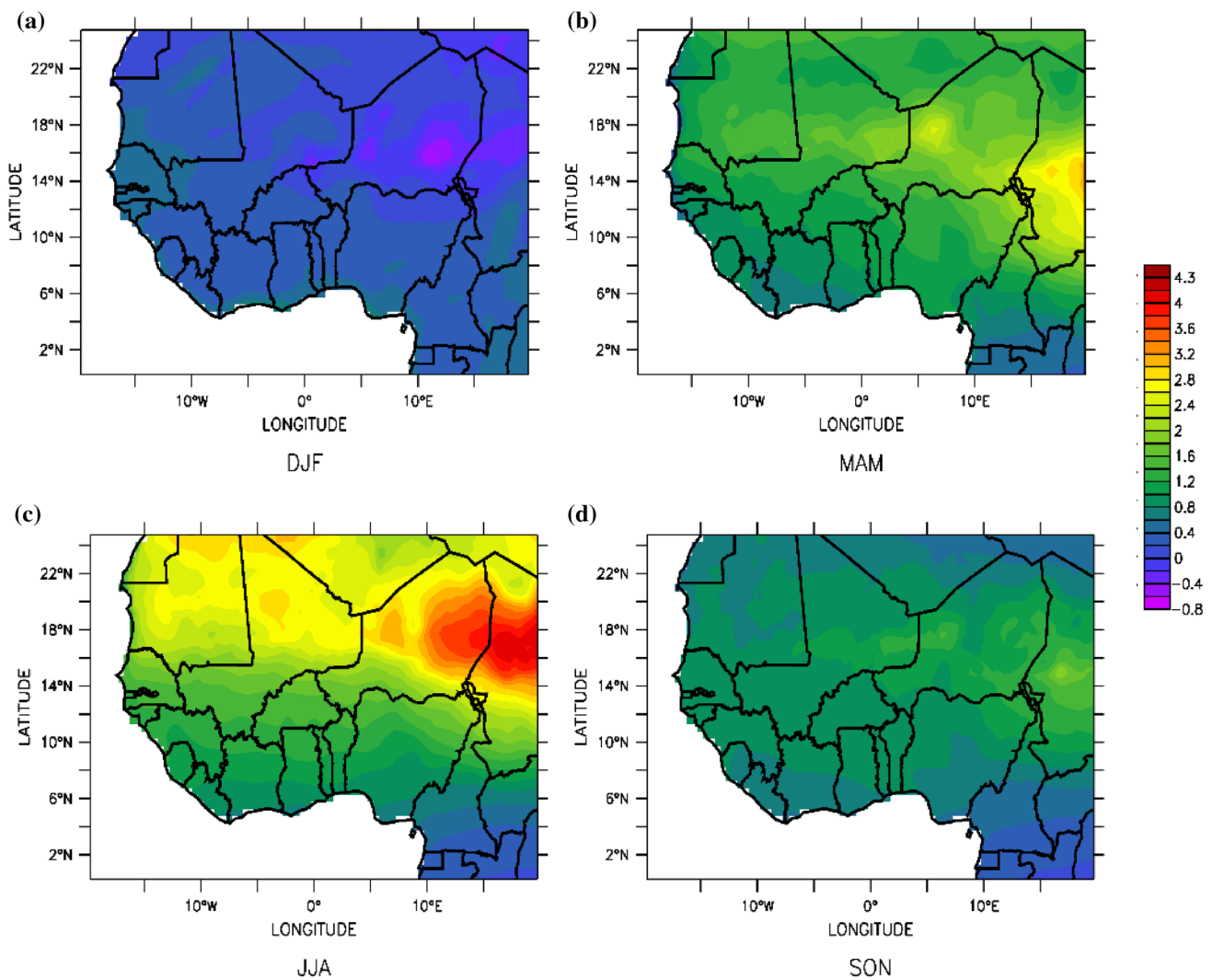
Fig. 11 Dust induced Longwave Radiative Forcing (W/m2) at the TOA for **a** DJF **b** MAM **c** JJA **d** SON for 2010

feedbacks (dust + rad). Other experiments were close to the observed in terms of standard deviation and RMSE which implies that, the experiments were significant in explaining the variations of rainfall over the Sahel. Generally, it is suggested that most of the experiments on RegCM4 performed very well thus, they can be used in explaining the spatial variability of rainfall over West Africa.

Intraseasonal variability of West African climate

The latitude-time cross-section of both modeled and observed mean rainfall over West Africa is shown in Figure (16). The monsoon flow migrates northward from 4°N to about 12°N from January to December. Figure 16(a–d) also revealed the onset of raining season in March. The period of the first raining season corresponds with the northward advancement of monsoon flow associated with ITD

between March and July with the peak in June, and the second raining season corresponds with the southward retreat of the flow between September and December with the core in October. A significant break (little dry season) experienced along the Guinea coast (south of 8°N) between July and September is associated with the further northward advancement of monsoon rainfall to about 12°N which brings high and one rainfall season over the Sahel (Diallo et al. 2012). However, the intensity and extent of dryness, and second wet season captured by TRMM observations (Fig. 17a) were not as profound as the modeled monsoon rainfall (Fig. 17b–c) over the Guinea coast. The southward shift of the rain band from September brings about a decrease in the rainfall intensity over the Sahel. Comparatively, RegCM4 tends to overestimate rainfall especially during the southward retreat of the monsoon, which is characterized as second wet season around September. In the
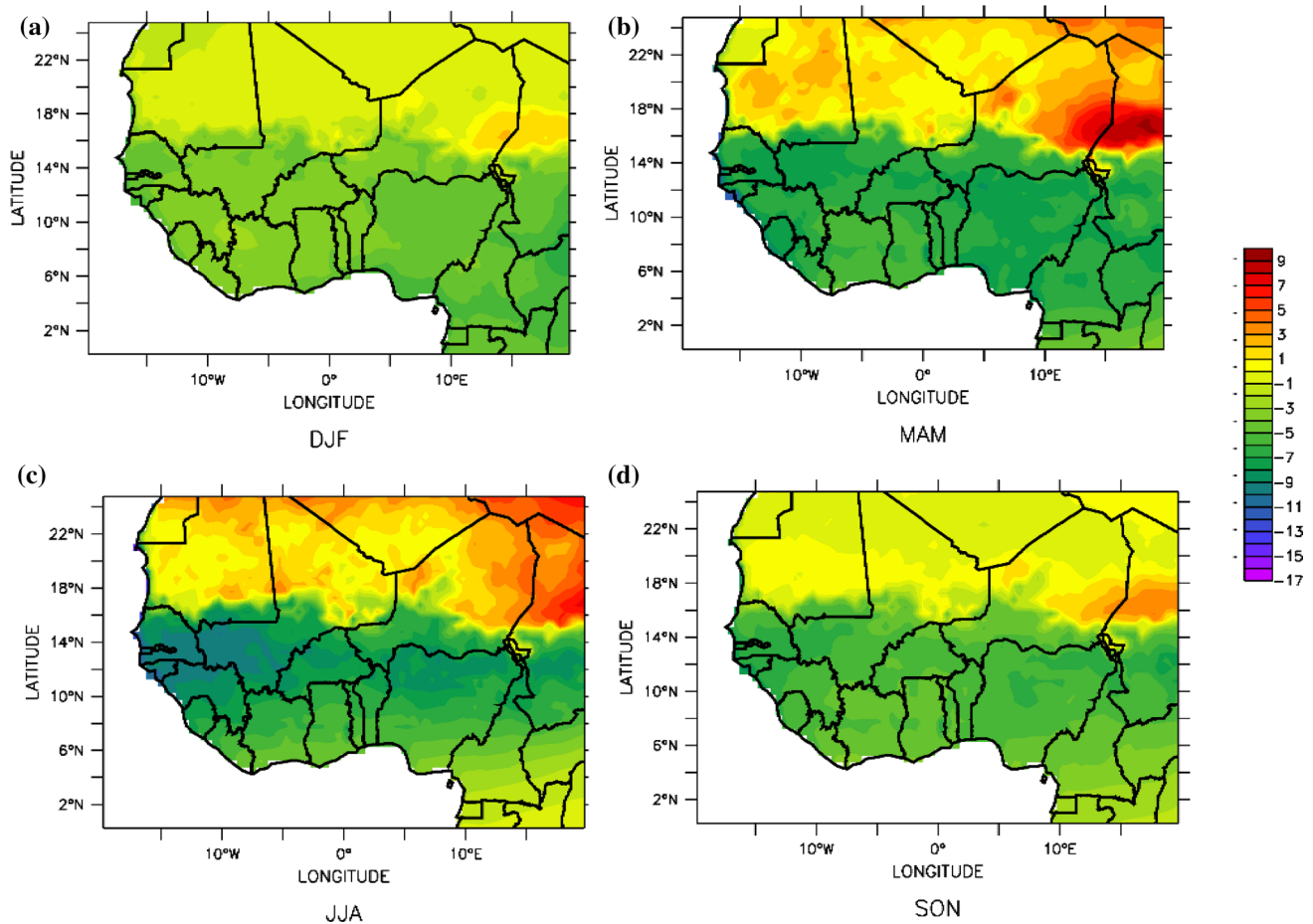
Fig. 12 Dust induced Net Radiative Forcing (W/m2) at the TOA for **a** DJF **b** MAM **c** JJA **d** SON for 2010

dust experiment, the simulated amount of rainfall (Fig. 17b, c) is generally lower in most of the regions south of 8°N, compared to the control run (Fig. 17b). This implies that the larger rainfall amount simulated in the control experiment is in line with improved performance on the part of the regional climate model. Therefore, the removal of dust in the regional climate model simulation reduces the dry bias found in the control simulation, leading to a more realistic rainfall distribution in West Africa. Over the Guinea coast, the TRMM shows two peaks of rainfall, a primary maximum in June, and a secondary maximum in October. A relative mid-summer break characterized as low rainfall was also observed in August as the rain band shifts northward in the Guinea coast. Due to the improved performance of RegCM4, no difference was found between the TRMM and model outputs except during the mid-summer break where the RegCM4 output showed underestimation of mean monthly rainfall in this zone. However, one significant fact observed in the Guinea coast is that RegCM4 captures the timing of the primary and secondary peaks, and mid-summer break perfectly well, as shown in Fig.

(17). This significant variation in the secondary maximum of mean monthly rainfall simulated by RegCMs might be related to their different sensitivities of radiative response based on the influx of moisture from the Atlantic (Thorncroft et al. 2011).

The period of raining season extends from June to September in all the datasets in the Savannah. Unlike the Guinea coast, rainfall pattern over Savannah zone showed unimodal with the peak occurring in August for the TRMM while that of RegCM outputs shift to the month of September (Fig. 17b). The RegCMs also showed overestimation in rainfall amount during the summer months in this zone.

Similarly, the rainfall pattern is also unimodal over the Sahelian zone with the peak well captured in the month of August for all the datasets (Fig. 17c). The period of the wet season is also less than four months from July to September in this zone. The RegCM4 control and dust without radiation feedbacks runs showed a slight overestimation of rainfall maximum when compared with TRMM observations. However, the rainfall output from RegCM4 dust with radiation feedbacks underestimated rainfall in
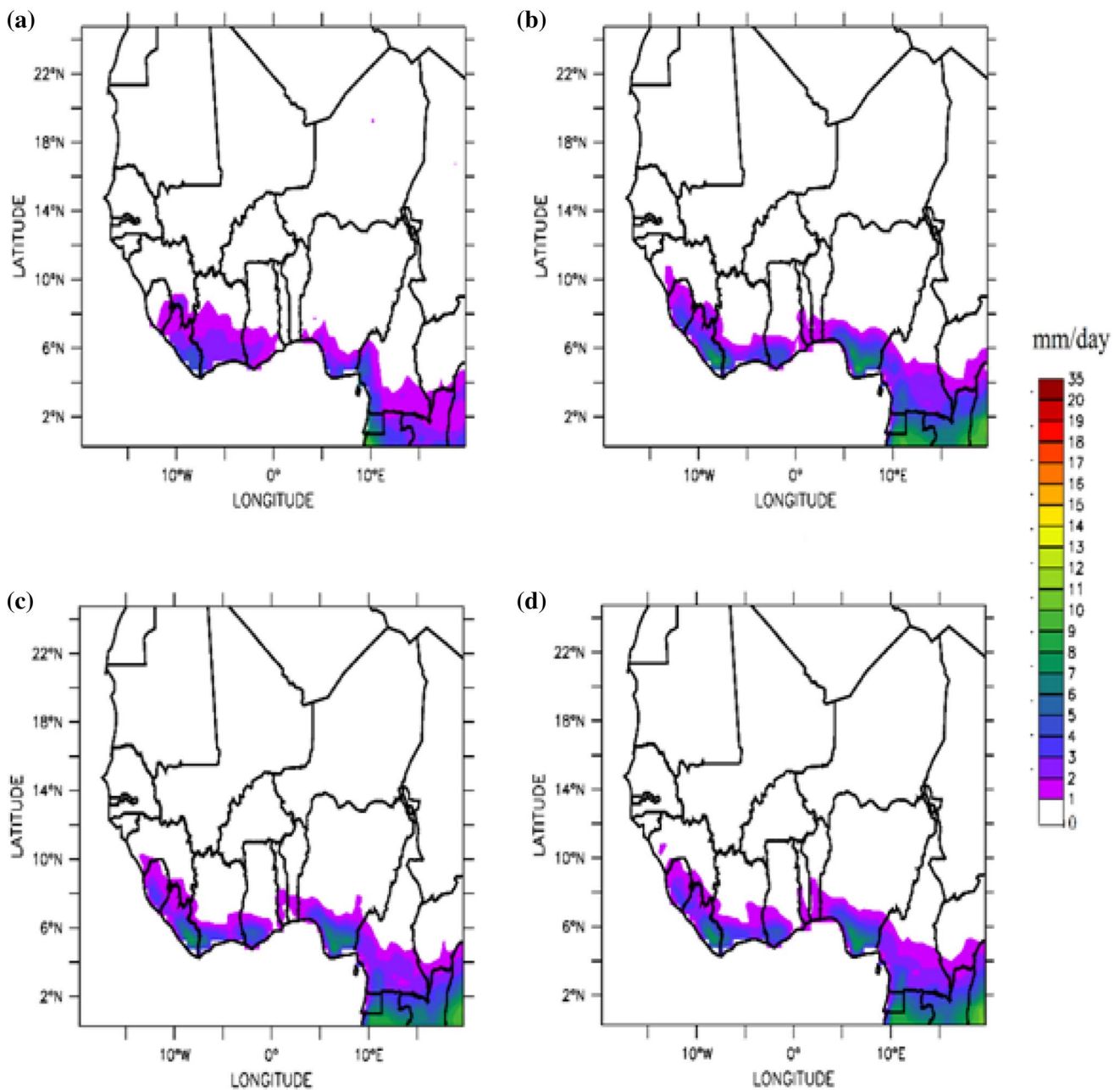
Fig. 13 Spatial distribution of precipitation over West Africa during the months of December-February, 2010 for **a** TRMM **b** RegCM control **c** RegCM dust with radiation feedbacks **d** RegCM dust without radiation feedbacks

the summer months between June and September over the Sahel (Fig. 17c).

The study further examined the main mechanisms driving the large scale features associated with WAM dynamics and convective activity in the summer season over West Africa (Fig. 18). The output exhibit a stratified structure of atmospheric circulation locating the monsoon flow (3–18°N) and harmattan fluxes (above 18°N) at low level between the surface and 850 hpa, the

African Easterly Jet (AEJ) is located in the mid-level at about (600–700 hpa) centered at between 12–16°N and the Tropical Easterly Jet (TEJ) in the upper troposphere at 200 hpa with the core of maximum wind at 10°N. The AEJ appears over West Africa during the boreal summer as a result of the strong meridional surface moisture and temperature gradients between the hot Sahara and the Atlantic Ocean which is characterized by moist convection to the south and dry convection to
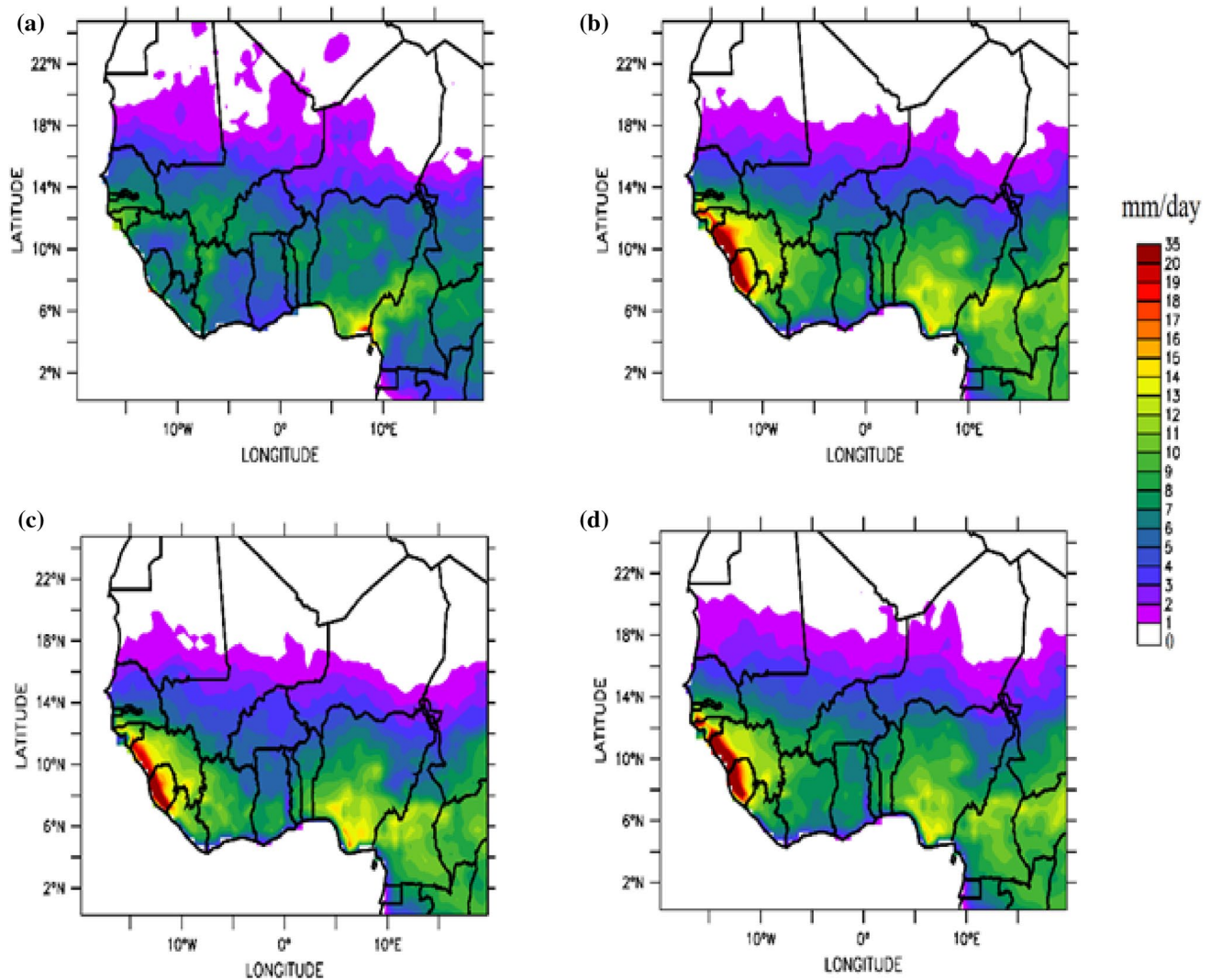
Fig. 14 Spatial distribution of precipitation over West Africa during June–September months of 2010 for **a** TRMM **b** RegCM control **c** RegCM dust with radiation feedbacks **d** RegCM dust without radiation feedbacks

the north (Thorncroft and Blackburn 1999; Cook 1999). The RegCMs also captured the structure of the features (Fig. 19c–d), the monsoon flow and the associated westerlies are well simulated both in depth and northward extent. The AEJ also showed a similar pattern in terms of the speed but a slight shift of the core northward. For the Upper- level jet, the RegCMs significantly reproduced the strength, location, and depth of the TEJ. The result of this work has shown that the contribution of dust to drier conditions over Sahel is related to the southward shift of AEJ which coincides with both weaker than normal TEJ and monsoon flux (Grist and Nicholson 2001). The findings showed the capability of RegCM4 in reproducing regional climatic features associated with WAM over West Africa.

Comparative analysis between of model and satellite observations

The relationship between RegCM4 simulated columnar AOD with observed AERONET AOD, MODIS-TERRA, MISR, and OMI at selected stations under study was assessed based on the results obtained from the correlation analysis. Figure (19) shows that, the correlation coefficients (r) between AOD simulated by RegCM4 and AERONET, MODIS-TERRA, MISR, and OMI for Dakar were 0.64, 0.76, 0.86, and 0.58 respectively. Banizoumbou showed good correlation (r = 0.59, 0.52, and 0.78) between RegCM AOD, AERONET, MISR and OMI respectively. However, a poor correlation (r < 0.5) was found over Banizoumbou
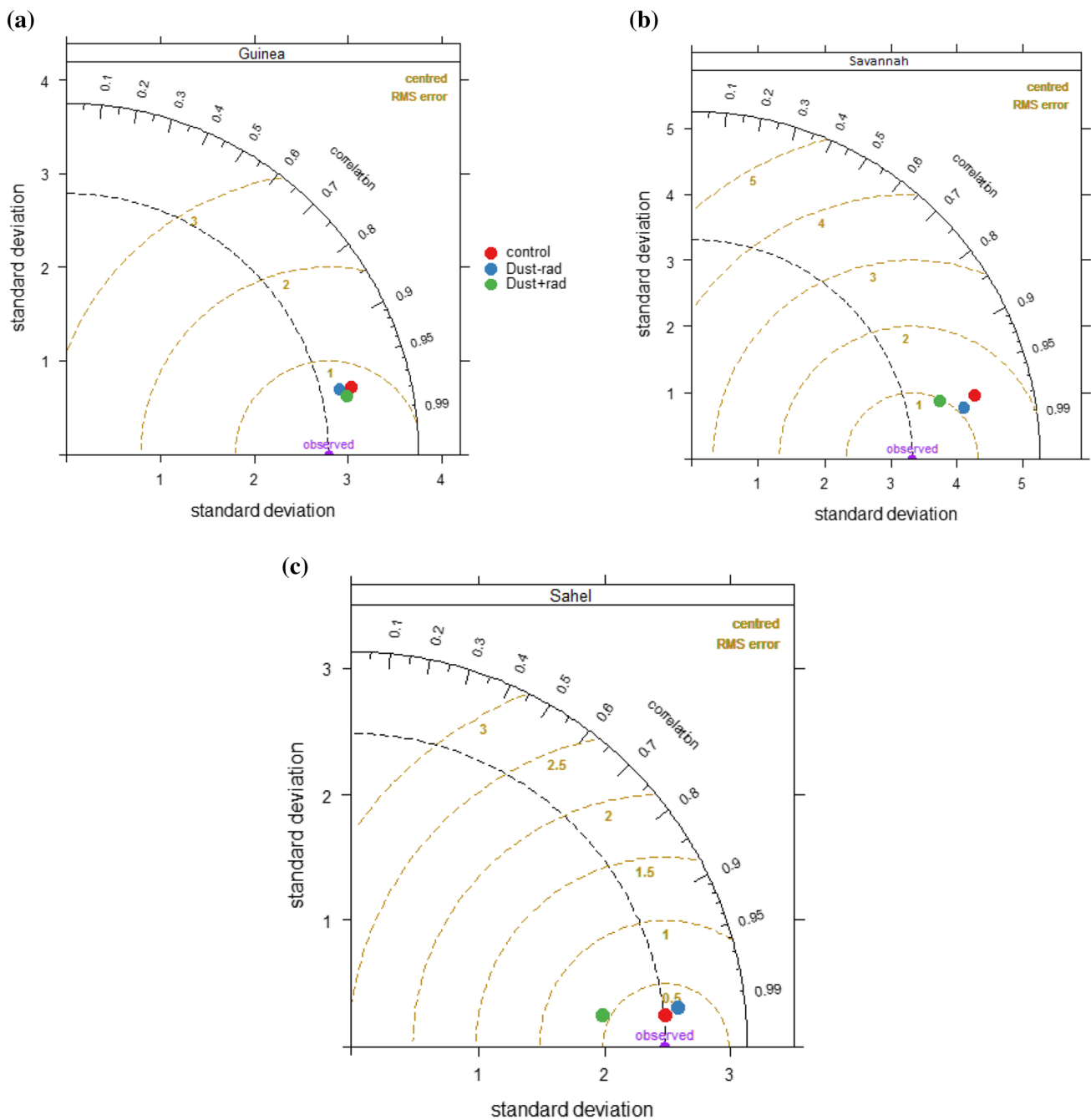
Fig. 15 Taylor's diagram for TRMM and RegCMs over **a** Guinea and **b** Savannah **c** Sahel

when RegCM4 simulation was compared with MODIS-TERRA. Cape Verde showed the highest correlation (r > 0.7) for the ground and all the satellite observations (Fig. 19). This implies that the model performs very well in reproducing dust outflow over tropical Atlantic Ocean than the continental locations of the region. The RegCM4 simulated AOD showed poor relationship with satellite

observations in other stations used in this study (Figs. 20, 21), which might be as a result of sparse data distribution over these stations. These findings are consistent with studies which suggested that models were able to better reproduce trans-atlantic dust transport and perform better during boreal summer than winter (Kim et al. 2014; Huneeus et al. 2011). In general, it was found that, the RegCM4 simulated
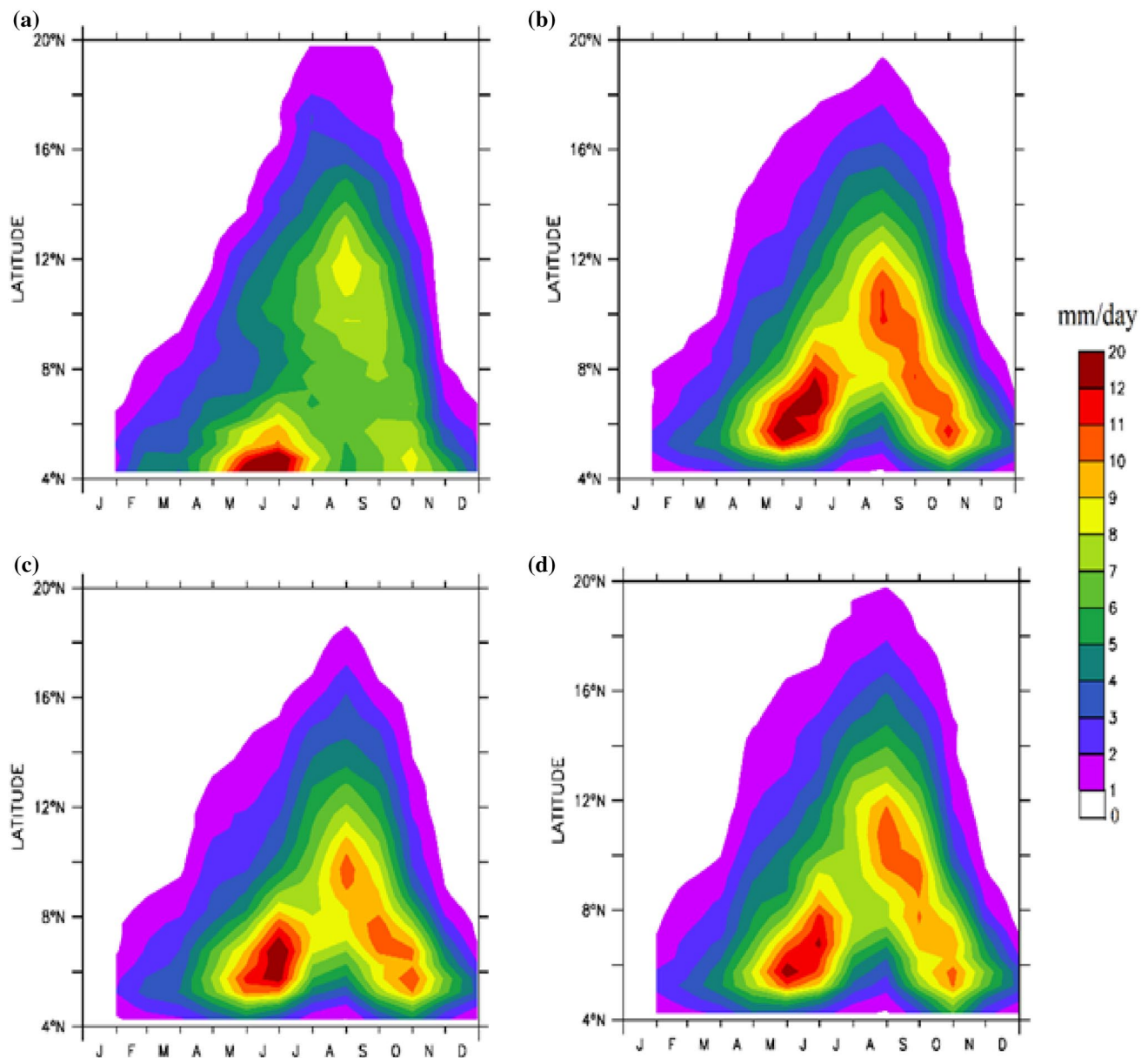
Fig. 16 Latitude-time cross section of mean daily precipitation (mm/day) for **a** TRMM **b** RegCM control **c** RegCM dust with radiation feedbacks **d** RegCM dust without radiation feedbacks; for 2010

results conformed with ground AERONET, MISR and OMI (between 40 and 90%) observations than MODIS-TERRA observations at most locations over West Africa.

Conclusion

The study aimed at investigating the radiative effects of dust aerosol on West African climate using a regional climate model (RegCM4.4) developed by the ICTP. The

simulations was performed with the non-aerosol version of the model (control) and a dust module for the year 2010. The model outputs were compared with observation, satellite and reanalysis data. The main findings can be summarized as follows:

1. The RegCM4 exhibited a remarkable performance in capturing the major aerosol source regions over the study area. The Bodele depression which extend from Niger to Chad had the highest dust concentration and
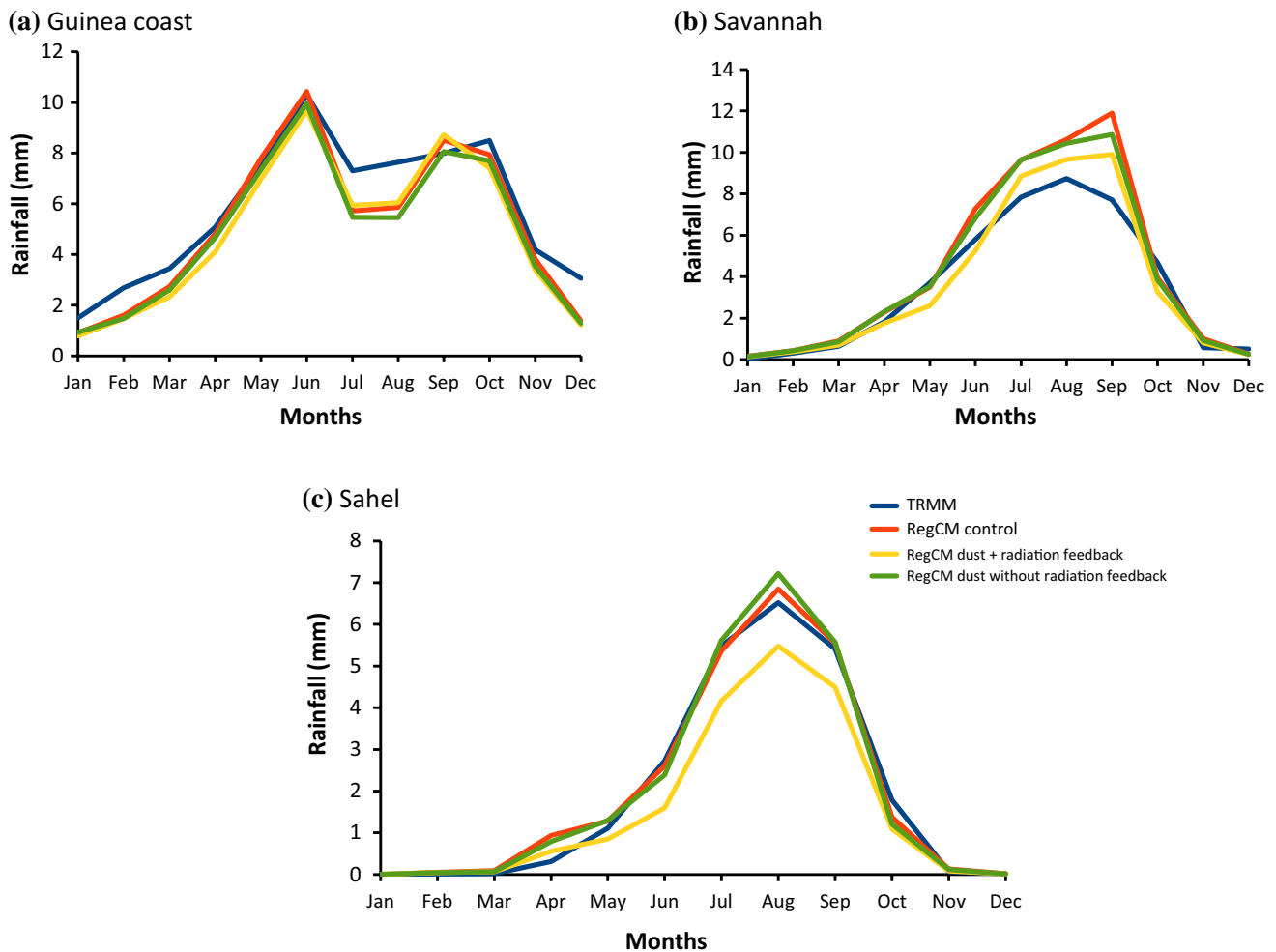
(a) Guinea coast

(b) Savannah

(c) Sahel

- TRMM
- RegCM control
- RegCM dust + radiation feedback
- RegCM dust without radiation feedback

Fig. 17 Zonal variation of mean monthly rainfall (mm) for TRMM; RegCM control; RegCM dust with radiation feedbacks and; RegCM dust without radiation feedbacks over **a** Guinea coast **b** Savannah **c** Sahel

emissions over the study area with maximum activity in the month of March.

2. The dust wet deposition occur only during the rainy months and it's driven by the dynamics of the ITD.

3. During the study period of 2010, large variations in the distribution of dust aerosol particles was observed majorly in three locations. Banizoumbou with maximum AOD loading on the 26th March and 5th April; Cape Verde showed the maximum AOD in 11th June while, that over Dakar was observed on the 9th March and 2nd May.

4. During the observed days of maximum AOD, result from the hysplit backward trajectories model showed that the air masses reaching Dakar and Cape Verde from the lowest level (i.e. 500 m up to 2000 m) originated from the Senegal, Mauritania, and Mali areas.

While at high altitude (from 3000 m and beyond), long-range aerosol particles ending at these stations originated from the Mediterranean Sea. In contrast, the lower level air masses reaching Banizoumbou and Ilorin originated mainly from the Sahara desert of northern Africa which has been identified as the major source region of dust loads.

5. The negative values observed in SWSRF and NSRF indicated that dust aerosol exerts essentially a cooling effect in all seasons over West Africa, with maximum impacts during the JJA.

6. In the atmosphere, the shortwave (longwave) dust aerosol radiative effect exerted a warming (cooling) effect over the study area while a reversal was evident at the surface. The overall net radiative effects (i.e. longwave–shortwave) of dust aerosol over West Africa is
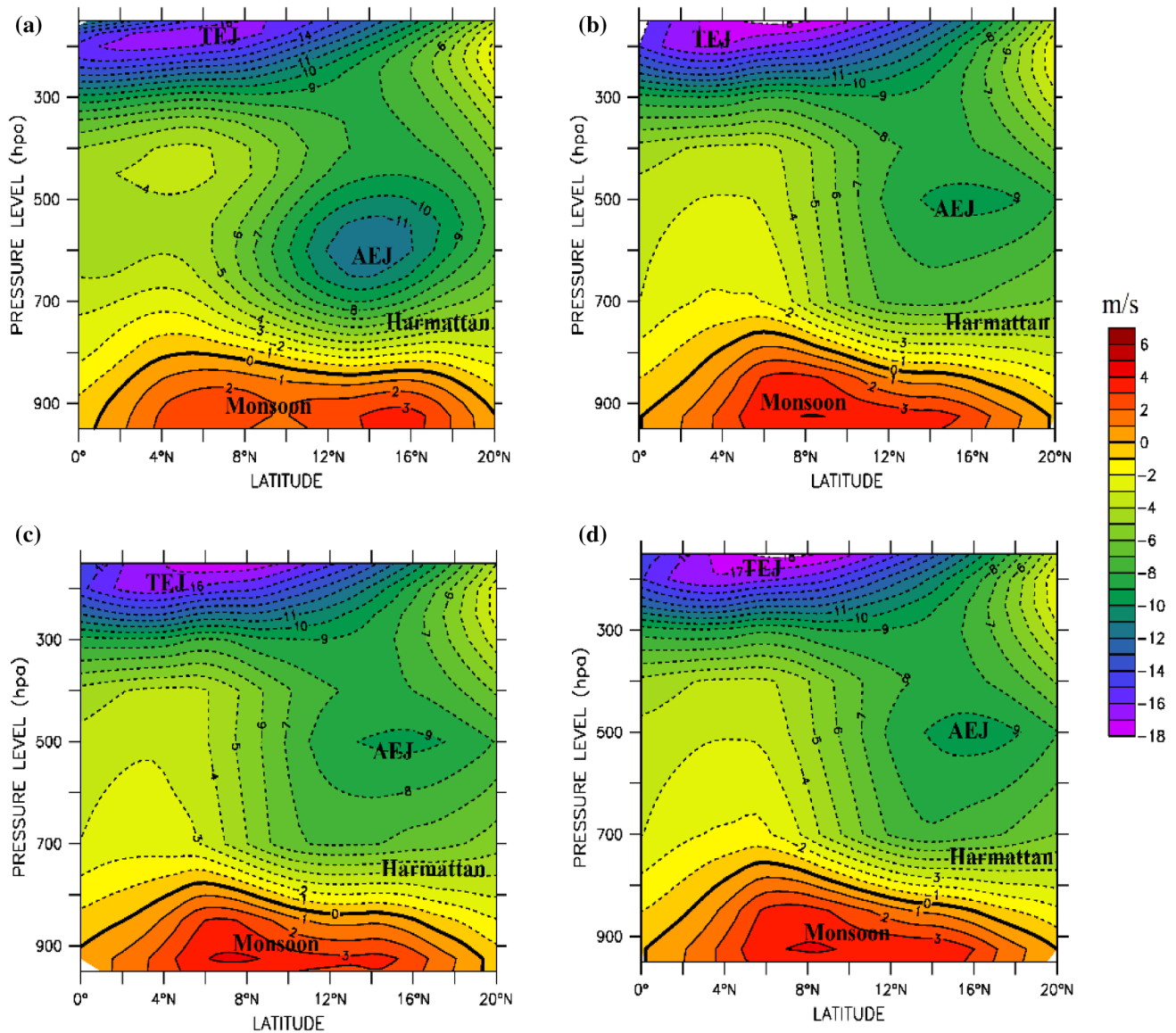
Fig. 18 The vertical cross section of zonal wind (m/s) over West Africa for **a** Era Interim **b** RegCM control **c** RegCM dust with radiation feedbacks **d** RegCM dust without radiation feedbacks for 2010

therefore; an atmospheric warming, surface cooling and a relatively small anomalous effect at the top of the atmosphere.

7. The model skillfully reproduced the rainfall distribution and amounts over the study area, although with differing level of accuracy. In addition, the dust induced runs overestimated orography related rainfall over the Guinea highlands and Jos plateau.

8. The dust aerosol runs simulated a weakened monsoon flow over the Sahel in coherence with the magnitude, position and intensity of the African Easterly Jet and Tropical Easterly Jet and thus, resulting to an obvious decline in Sahel rainfall.

9. The RegCM4 simulated aerosol optical depth exhibited a good positive realtionship with both the observation and satellite products in majority of the stations considered.

Fig. 19 Comparison of RegCM and observed MODIS, MISR, OMI, and AERONET AOD over Dakar, Banizoumbou, and Cape Verde in West Africa
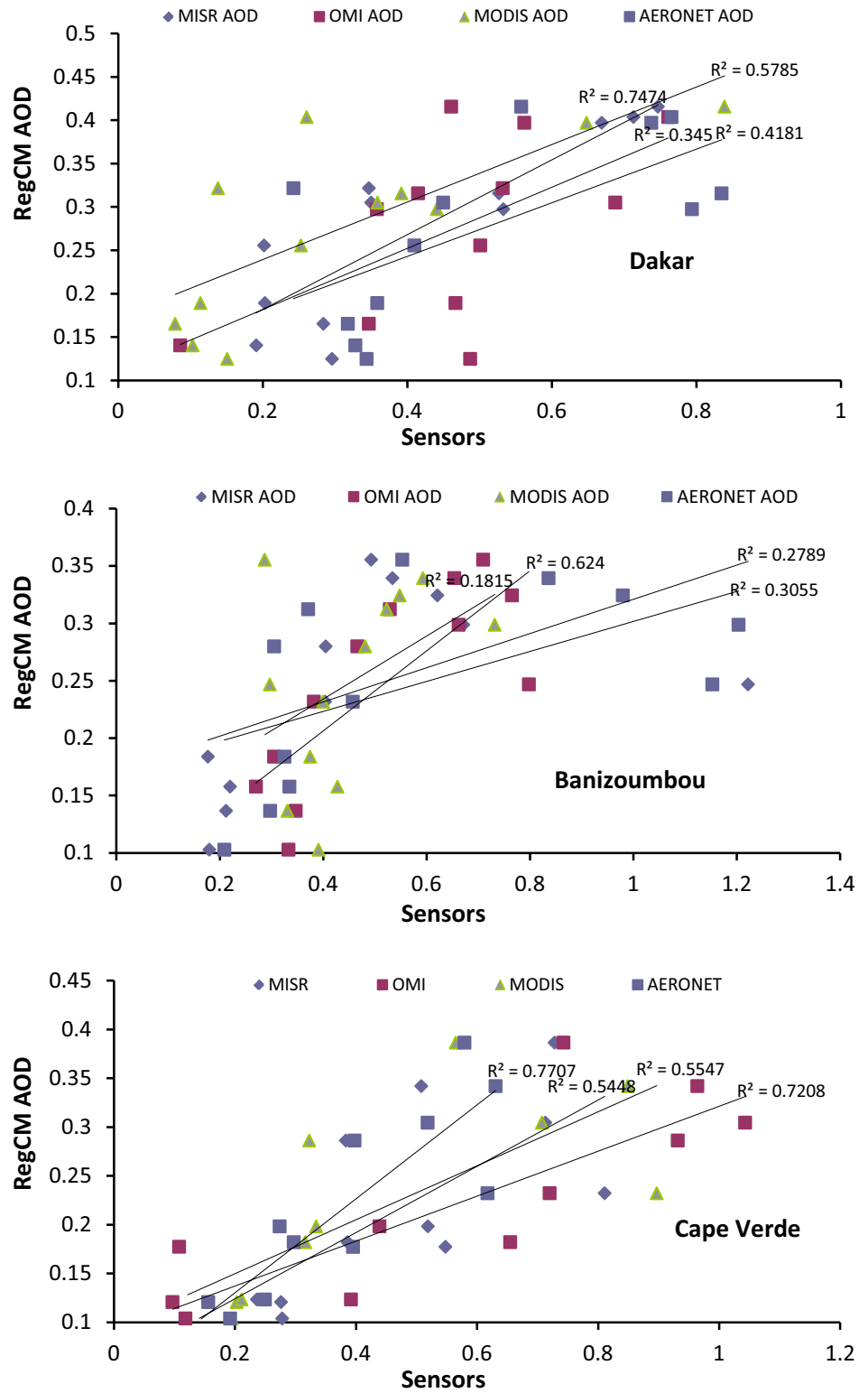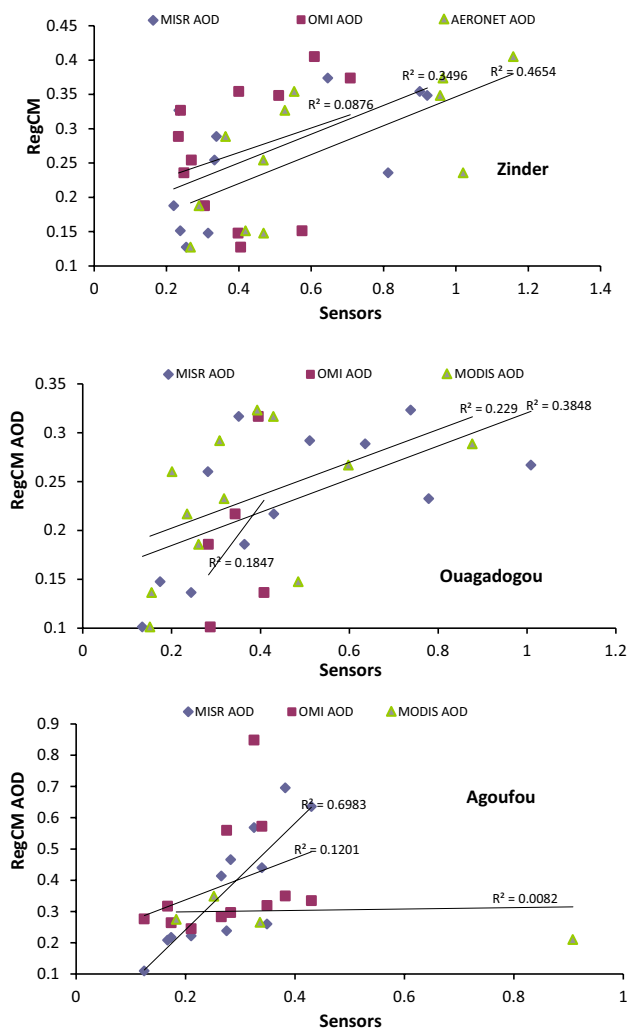
Fig. 20 Comparison of RegCM and observed MODIS, MISR, OMI, and AERONET AOD over Zinder, Ouagadogou, and Agoufou in West Africa
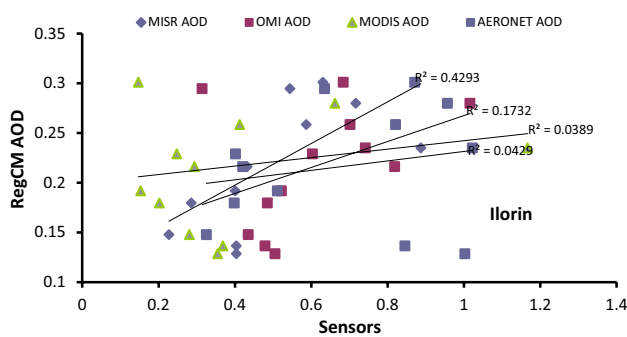

Fig. 21 Comparison of RegCM and observed MODIS, MISR, OMI, and AERONET AOD over Ilorin in West Africa

References

Abiodun BJ, Adeyewa ZD, Oguntunde PG, Salami A, Ajayi VO (2012) Modeling the impacts of reforestation on future climate in West Africa. Theor Appl Climatol 110(1–2):77–96

Adeyewa ZD, Nakamura K (2003) Validation of TRMM radar rainfall data over major climatic regions in Africa. J Appl Meteor 42:331–347

Akinsanola AA, Ogunjobi KO, Gbode IE, Ajayi VO (2015) Assessing the capabilities of three regional climate models over CORDEX Africa in simulating West African summer monsoon precipitation. Adv Meteorol 2015: 935431. doi:10.1155/2015/935431

Chiapello I, Bergametti G, Gomes L, Chatenet B, Dulac F, Pimenta J, Suares ES (1995) An additional low layer transport of Sahelian and Saharan dust over the north-eastern Tropical Atlantic. Geophys Res Lett. doi:10.1029/95GL03313.

Cook KH (1999) Generation of the African easterly jet and its role in determining West African precipitation. J Climate 12:1165–1184, doi:10.1175/15200442

Croft B, Pierce JR, Martin RV, Hoose C, Lohmann U (2012) Uncertainty Associated with convective wet removal of entrained aerosols in a global climate Model. Atmos Chem Phys 12:10725–10748

Darmenova K, Sokolik IN (2007) Assessing uncertainties in dust emission in the Aral Sea region caused by meteorological fields predicted with a mesoscale model. Glob Planet Change 56:297–310. doi:10.1016/j.gloplacha.2006.07.024

Darmenova K, Sokolik IN, Shao Y, Marticorena B, Bergametti G (2009) Development of a physically based dust emission module within the Weather Research and Forecasting (WRF) model: assessment of dust emission parameterizations and input parameters for source regions in Central and East Asia. J Geophys Res 114:D14201. doi:10.1029/2008JD011236

Diallo I, Sylla MB, Giorgi F, Gaye, AT, Camara M (2012) Multi-model GCM-RCM ensemble based projections of temperature and precipitation over West Africa for the early 21st century. Int J Geophys. doi:10.1155/2012/972896

Ginoux P, Garbuzov D, Hsu NC (2010) Identification of anthropogenic and natural dust sources using Moderate Resolution Imaging Spectroradiometer (MODIS) Deep Blue level 2 data. J Geophys Res 115:D05204. doi:10.1029/2009JD012398

Ginoux P, Prospero J, Gill TE, Hsu NC, Zhao M (2012) Global scale attribution of anthropogenic and natural dust sources and their emission rates based on MODIS deep blue aerosol products. Rev Geophys. doi:10.1029/2012RG000388

Giorgi F, Coppola E, Solmon F, Mariotti L, Sylla M, Bi X, Elguindi N, Diro GT, Nair V, Giuliani G, Cozzini S, Guettler I, O'Brien T, Tawfik A, Shalaby A, Zakey AS, Steiner A, Stordal F, Sloan L, Brankovic C (2012) RegCM4: model description and preliminary tests over multiple CORDEX domains. Clim Res. doi:10.3354/cr01018

Gong SL, Zhang XY, Zhao TL, McKendry IG, Jaffe DA, Lu NM (2003) Characterization of soil dust aerosol in China and its transport and distribution during 2001 ACE-Asia: model simulation and validation. J Geophys Res 108(D9):4262. doi:10.1029/2002JD002633

Goudie AS, Middleton NJ (2001) Saharan dust storms: nature and consequences. Earth Sci Rev 56(1–4):179–204

Grist JP, Nicholson SE (2001) A study of the dynamic factors influencing the rainfall variability in the West African Sahel. J Clim 14(7):1337–1359

Gu Y et al. (2012) Dust aerosol impact on North Africa climate: a GCM Investigation of aerosol-cloud-radiation interactions using A-Train satellite data. Atmos Chem Phys 12:1667–1679. doi:10.5194/acp-12-1667-2012

Holben BN, Eck TF, Slutsker I, Tanre D, Buis JP, Setzer A, Vermote EF, Reagan JA, Kaufman YJ, Nakajima T, Lavenu F, Jankowiak I, Smirnov A (1998) AERONET – A federated instrument network and data archive for aerosol characterization. Remote Sens Environ 66:1–16

Holben BN, Tanre D, Smirnov A, Eck TF, Slutsker I, Abuhassan N, Newcomb WW, Schafer J, Chatenet B, Lavenue F, Kaufman YJ, Vande Castle J, Setzer A, Markham B, Clark D, Frouin R, Halthore R, Karnieli A, O'Neill NT, Pietras C, Pinker RT, Voss K, Zibordi G (2001) An emerging ground-based aerosol climatology: Aerosol optical depth from AERONET. J Geophys Res 106: 12067–12097

Huang JP, Fu Q, Su J, Tang Q, Minnis P, Hu Y, Yi Y, Zhao Q (2009) Taklimakan dust aerosol radiative heating derived from CALIPSO observations using the Fu-Liou radiation model with CERES constraints, Atmos. Chem Phys 9:4011–4021 doi:10.5194/acp-9-4011-2009

Huang JP, Minnis P, Yan H, Yi Y, Chen B, Zhang L, Ayers JK (2010) Dust aerosol effect on semi-arid climate over Northwest China detected from A-Train satellite measurements. Atmos Chem Phys 10:6863–6872. doi:10.5194/acp-10-6863-2010

Huffman GJ, Adler RF, Bolvin DT, Gu G, Nelkin EJ, Bowman KP, Hong Y, Stocker EF, Wolff DB (2007) The TRMM multisatellite precipitation analysis (TMPA): quasi-global, multiyear, combined sensor precipitation estimates at fine scales. J Hydrometeorol 8(1):38–55. doi:10.1175/JHM560.1

Huffman GJ, Adler RF, Morrissey M, Bolvin D, Curtis S, Joyce R, McGavock B, Susskind J (2001) Global precipitation at one-degree daily resolution from multisatellite observations. J Hydrometeor 2:36–50

Huneeus N, Dentener F, Diehl T, Easter R, Fillmore D (2011) Global dust model intercomparison in AeroCom phase I. Atmos Chem Phys 11(15):7781–7816. doi:10.5194/acp-11-7781-2011

Kaufman YJ, Tanre D, Remer LA, Vermote EF, Chu A, Holben BN (1997) Operational remote sensing of tropospheric aerosol over land from EOS moderate resolution imaging spectroradiometer. J Geophys Res 102:17051–17067

Kim D, Chin M, Yu H, Diehl T, Tan Q, Kahn RA, Koffi B (2014) Sources, sinks, and transatlantic transport of North African dust aerosol: A multimodel analysis and comparison with remote sensing data. J Geophys Res 119(10):6259–6277

Klüser L, Holzer-Popp T (2010) Relationships between mineral dust and cloud properties in the West African Sahel. Atmos Chem Phys 10:6901–6915

Konare A, Zakey AS, Solmon F, Giorgi F, Rauscher S, Ibrah S, Bi X (2008) A Regional Climate modeling study of the effect of desert dust on the West African monsoon. J Geophys Res 113:D12206. doi:10.1029/2007JD009322

Mahowald N, Albani S, Engelstaedter S, Winckler G, Goman M (2011) Model insight into glacial-interglacial paleodust records. Quat Sci Rev 30(7–8):832–854

Malavelle F, Pont V, Mallet V (2011) Simulation of aerosol radiative effects over West Africa during DABEX and AMMA SOP-0. J Geophys Res D 116(8):D08205

McTainsh GH, Leys JF, Nickling WG, (1999) Wind erodibility of arid lands in the Channel Country of western Queensland, Australia. Zeitschrift für Geomorphologie N.F. 116, 113–130

Miller RL, Perlwitz J, Tegen I (2004) Modeling Arabian dust mobilization during the Asian summer monsoon: the effect of prescribed versus calculated SST. Geophys Res Lett 31:L22214. doi:10.1029/2004GL020669

Ogunjobi KO, Kim YJ (2008) Aerosol characteristics and surface radiative forcing components during a dust outbreak Gwanju, Republic of korea. Environ Monit Assess 137(1–3):111–126

Omotosho JB, Abiodun BJ (2007) A numerical study of moisture build-up and rainfall over West Africa. Meteorol Appl 14:209–225

Ozer P (2001) Les lithometeores en region sahelienne. Int J Trop Ecol Geogr 24:1–317

Perlwitz, J, Tegen I, Miller RL (2010) Interactive soil dust aerosol model in the GISS GCM: 1. Sensitivity of the soil dust cycle to radiative properties of soil dust aerosols. J Geophys Res 106:18167–18192

Prospero JM (2002) Environmental characterization of global sources of atmospheric soil dust identified with the Nimbus 7 total ozone mapping spectrometer (TOMS) absorbing aerosol product. Rev Geophys 40(1):1002. doi:10.1029/2000RG000095

Rotstayn LD (2011) Simulated enhancement of ENSO-related rainfall variability due to Australian dust. Atmos Chem Phys 11:6575–6592. doi:10.5194/acp-11-6575-2011

Sajani S (2012) Monsoon sensitivity to aerosol direct radiative forcing in the community atmosphere model. J Earth Syst Sci 121(4):867–889

Shao Y, Wyrwoll KH, Chappell A, Huang J, Lin Z, Mctainsh GH, Mikami M, Tanaka TY, Wang X, Yoon S (2011) Dust cycle: an emerging core theme in Earth system science. Aeolian Res 2:181–204. doi:10.1016/j.aeolia.2011.02.001

Shi G, Wang H, Wang B, Li W, Gong S, Zhao T (2005) Sensitivity experiments on the effects of optical properties of dust aerosols on their radiative forcing under clear sky condition. J Meteorol Soc Jpn 83 A:333–346. doi:10.2151/jmsj.83A.333

Solmon F, Mallet M, Elguindi N, Giorgi F, Zakey A, Konare A (2008) Dust aerosol impact on Regional Precipitation over western Africa, mechanisms and sensitivity to absorption properties. Geophys Res Lett 35:L24705. doi:10.1029/2008GL035900

Solmon F, Elguindi N, Mallet M (2012) Radiative and climatic effects of dust over West Africa, as simulated by a regional climate model. Climate Res 52:97–113. doi:10.3354/cr01039

Tesfaye M, Botai J, Sivakumar V, Mengistu TG (2013) Evaluation of regional climatic model simulated aerosol optical properties over South Africa using ground-based and satellite observations. ISRN Atmos Sci 2013:17. doi:10.1155/2013/237483

Tesfaye M, Mengistu TG, Botai J, Sivakumar V, RCJ Dehl (2015) Mineral dust aerosol distributions, its direct and semi-direct effects over South-Africa based on regional climate model simulation. J Arid Environ 114:22–40. doi:10.1016/j.jaridenv.2014.11.002

Thorncroft CD, Blackburn M (1999) Maintenance of the African Easterly Jet. Q J R Meteorol Soc 125:763–786

Thorncroft CD, Nguyen H, Zhang C, Peyrille P (2011) Annual cycle of the West African monsoon: regional circulations and associated water vapour transport. Q J R Meteorolog Soc 137(654):129–147

Todd MC, BouKaram D, Cavazos C, Bouet C and others (2008) Quantifying uncertainty in estimates of Mineral dust flux: an intercomparison of model performance over the Bodélé Depression, northern Chad. J Geophys Res 113:D24107. doi:10.1029/2008JD010476

Tummon F (2011) Direct and Semi-direct aerosol effects on the Southern African regional climate during the Austral Winter season (Ph.D. thesis). University of Cape Town, South Africa

Tummon F, Solmon F, Liousse C, Tadross M (2010) Simulation of the direct and semi direct aerosol effects on the southern Africa regional climate during the biomass burning season. J Geophys Res 115:D19206. doi:10.1029/2009JD013738

Wang Y (2004) Regional climate modeling: progress, challenges, and prospects. J Meteor Soc Jpn 82:1599–1628

Washington R, Todd MC (2005) Atmospheric controls on mineral dust emission from the Bode´le´ Depression, Chad: the role of the low level jet. Geophys Res Lett 32:L17701. doi:10.1029/2005GL023597

Woodward S (2005) A simulation of the effect of climate change-induced desertification on Mineral dust aerosol. Geophys Res Lett 32:L18810. doi:10.1029/2005GL023482

Yue X (2009) Simulation of dust aerosol radiative feedback using the global transport model of dust: Dust cycle and validation. J Geophys Res 114:D10202. doi:10.1029/2008JD010995

Zakey AS, Solmon F, Giorgi F (2006) Implementation and testing of a desert dust module in a regional climate model. Atmos Chem Phys 6:4687–4704

Zhang Y (2010) Simulating climate-chemistry-aerosol-cloud-radiation feedbacks in continental U.S. using online-coupled WRF/chem. Atmos Environ 44(29):3568–3582

Zhang Y, Duliere V, Mote PW, Salathe EP Jr (2009) Evaluation of WRF and HadRM mesoscale climate simulations over the U.S. Pacific Northwest. J Climate 22:5511–5526. doi:10.1175/2009JCLI2875.1

Zhao C, Liu X, Ruby Leung L, Hagos S (2011) Radiative impact of mineral dust on monsoon precipitation variability over West Africa. Atmos Chem Phys 11:1879–1893